Cosmic-Ray Anisotropy: The Data

Stefan Westerhoff

University of Wisconsin–Madison

Sources of Galactic cosmic rays

APC, Paris - December 7-9, 2016

Cosmic Ray Energy Spectrum

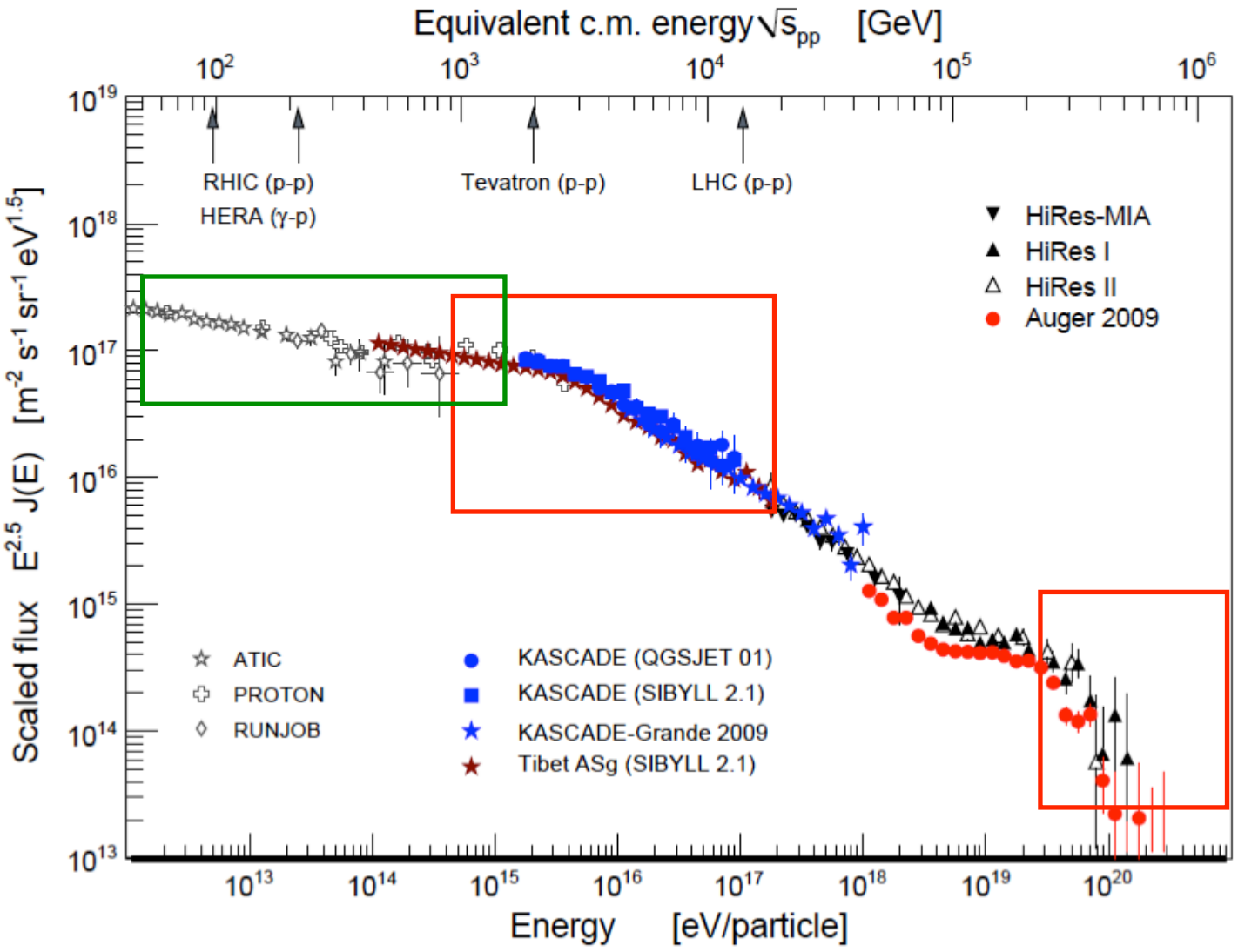

Unsmoothed Sky Maps

HAWC-100

D. Fiorino

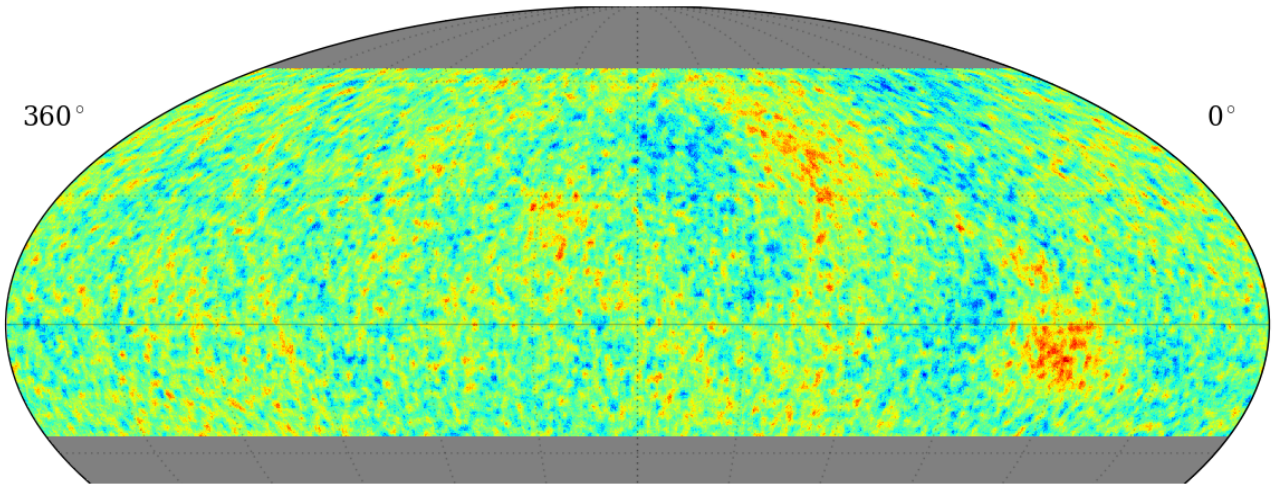

IceCube

ApJ 826 (2016) 220

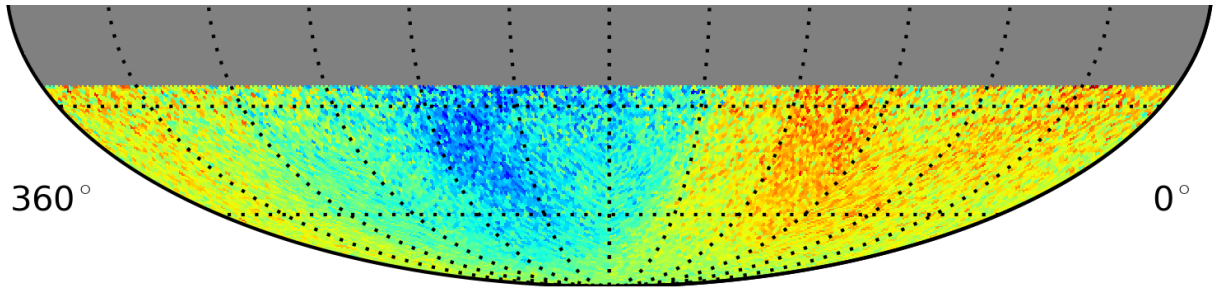

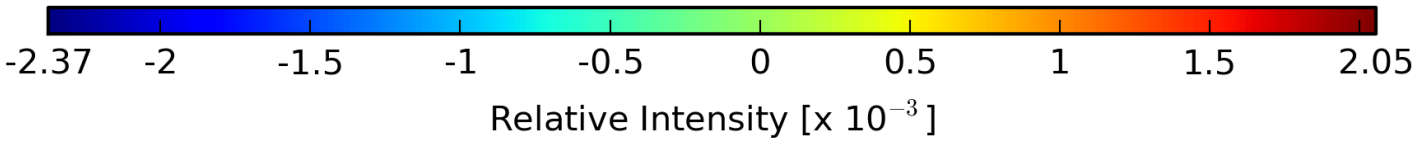

Angular Power Spectra

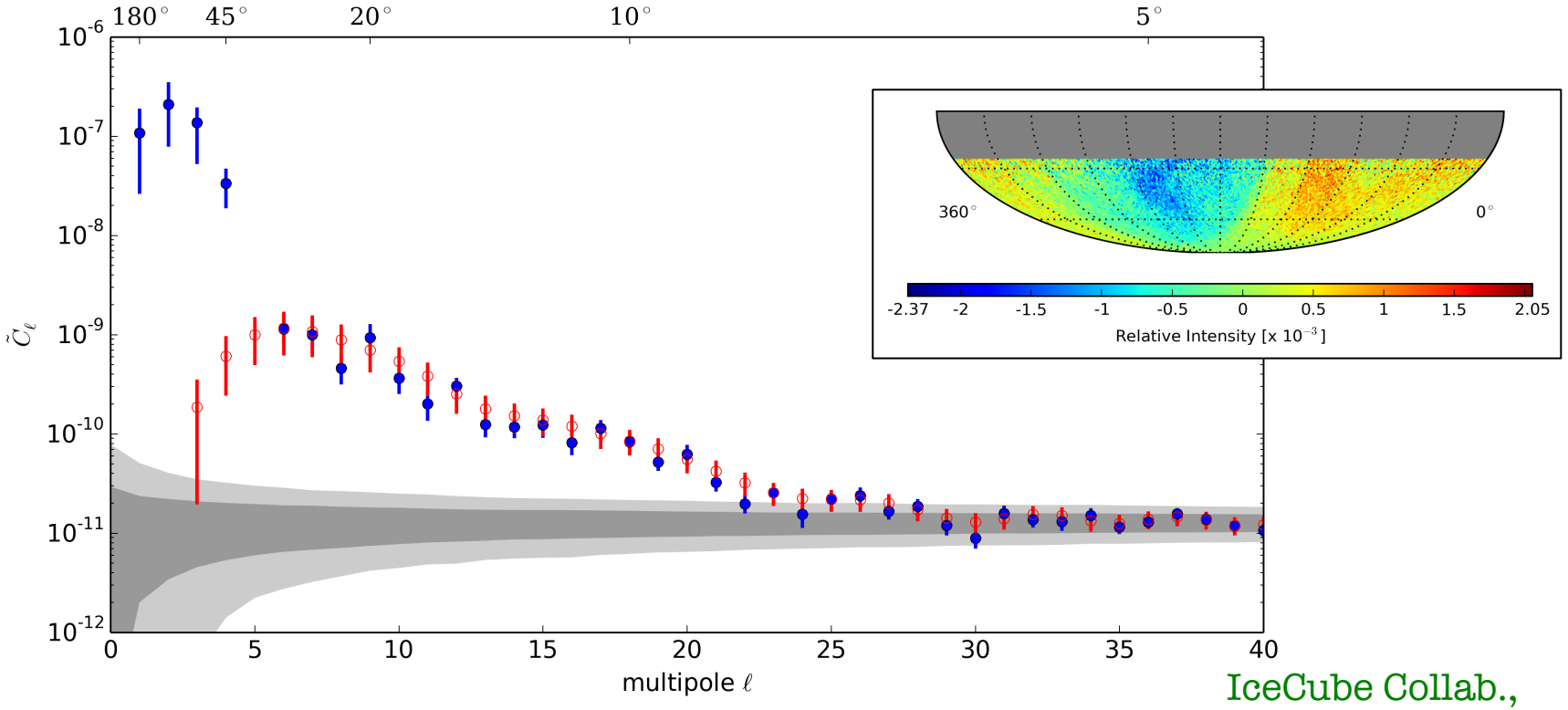

IceCube Collab.,
ApJ 826 (2016) 220

- Power spectrum for 6 years of IceCube data (*blue*).
- With best-fit dipole and quadrupole moments subtracted (*red*).
- Dark/light-gray bands represent isotropic flux at the 68% and 95% confidence levels.

Cosmic-Ray Anisotropy

- Cosmic-ray arrival direction anisotropy has been observed at high statistical significance by various surface and underground detectors, together covering an energy range from tens of GeV to tens of PeV.

- Large-scale structure (>60°) with relative intensity 10^{-3} .
  - Result of diffusive propagation?

- Small-scale structure also present, relative intensity 10^{-4} to 10^{-5} .

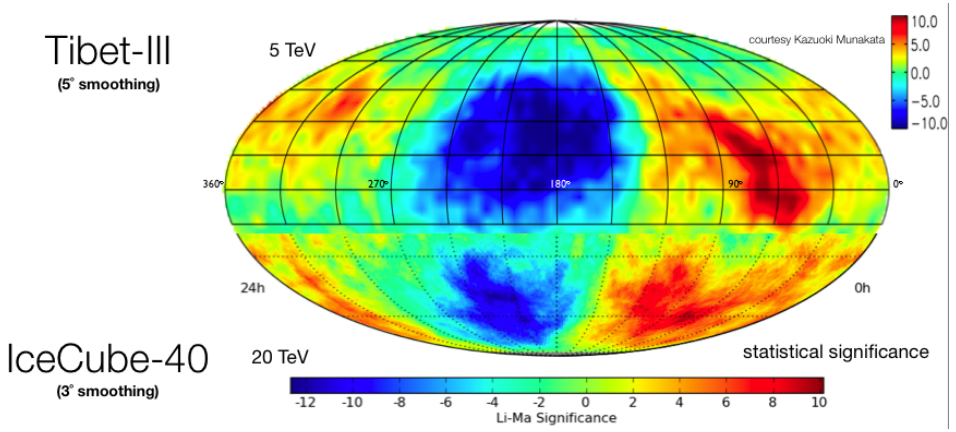

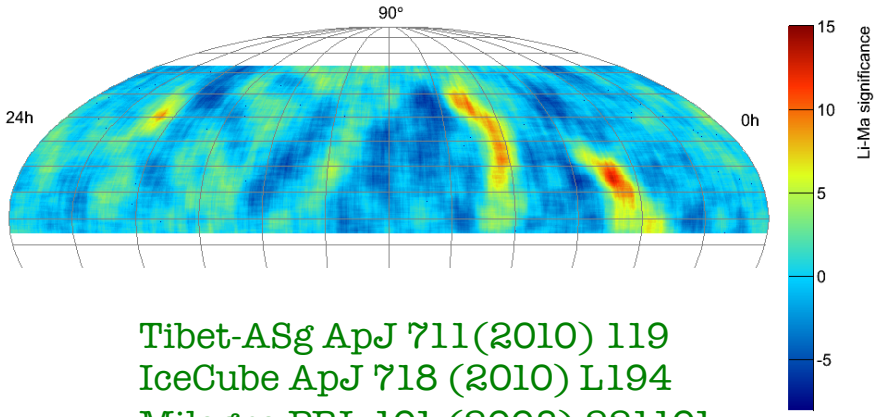

Tibet-ASg ApJ 711(2010) 119
IceCube ApJ 718 (2010) L194
Milagro PRL 101 (2008) 221101

Tibet ASγ, SuperKamiokande, Milagro, EAS-TOP, MINOS, ARGO-YBJ, HAWC, IceCube

Analysis Strategy

- Relative cosmic-ray intensity

$$I(\vec{n}) = \frac{\Phi(\vec{n})}{\Phi_{iso}}$$

data map

reference map

- The reference map represents the detector response to an isotropic cosmic-ray flux. Due to detector effects and diurnal and seasonable variations, the reference map is not in itself isotropic.
- Detector simulations are currently not accurate at the required level of 10^{-4} or less, so the reference map is typically reconstructed from the data.
  - Time-scrambling: generating "fake" events from the same local arrival direction distribution and the same event time distribution as the data.

    Alexandreas et al., NIM A 328 (1993) 570

  - Direct integration: rate of events observed in the detector as a function of local sidereal time is integrated against the relative acceptance during an integration period Δt
    - Integration time Δt averages arrival directions over 15° × (Δt /1 hr)

    Atkins et al., ApJ 595 (2003) 803

Biases of the Analysis Techniques

All detectors:

- Time scrambling and direct integration are equivalent to modifying the right ascension of the event within the same declination band.
  - Relative intensity maps are re-normalized in each declination band and show, by definition, equal contributions from *excesses* and *deficits*.
  - The methods are sensitive to anisotropy in right ascension, but insensitive to variations across declination bands, so any structure is effectively reduced to its projection onto right ascension.

Biases of the Analysis Techniques

All detectors:

- Time scrambling and direct integration are equivalent to modifying the right ascension of the event within the same declination band.
  - Relative intensity maps are re-normalized in each declination band and show, by definition, equal contributions from *excesses* and *deficits*.
  - The methods are sensitive to anisotropy in right ascension, but insensitive to variations across declination bands, so any structure is effectively reduced to its projection onto right ascension.

True injected signal

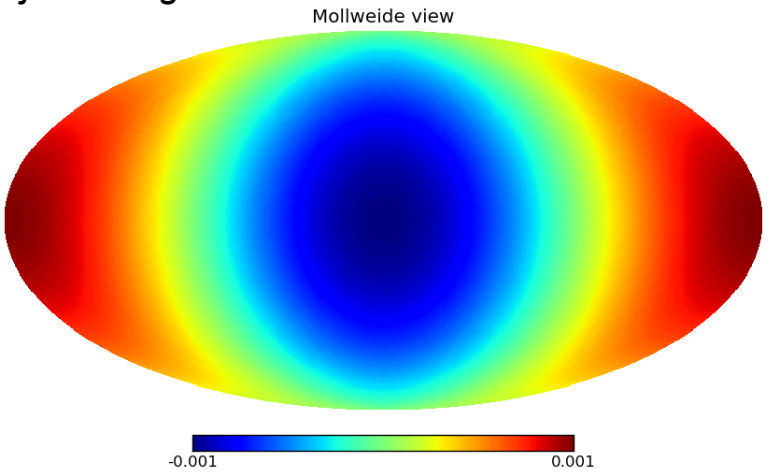

Reconstructed signal

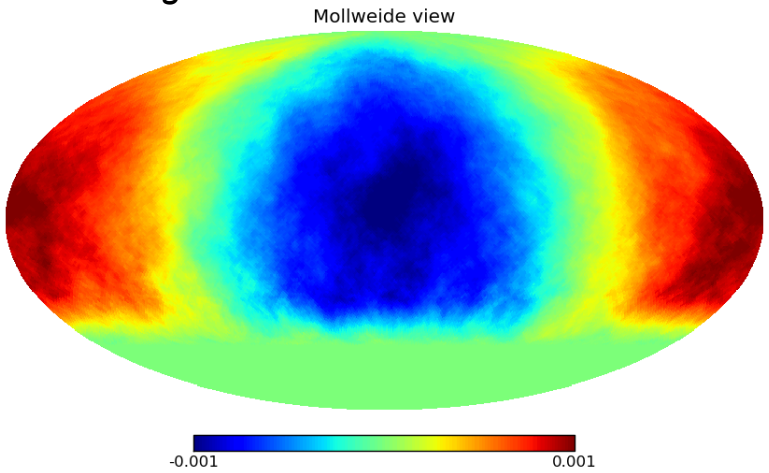

Dan Fiorino

Biases of the Analysis Techniques

All detectors:

- Time scrambling and direct integration are equivalent to modifying the right ascension of the event within the same declination band.
  - Relative intensity maps are re-normalized in each declination band and show, by definition, equal contributions from *excesses* and *deficits*.
  - The methods are sensitive to anisotropy in right ascension, but insensitive to variations across declination bands, so any structure is effectively reduced to its projection onto right ascension.

True injected signal

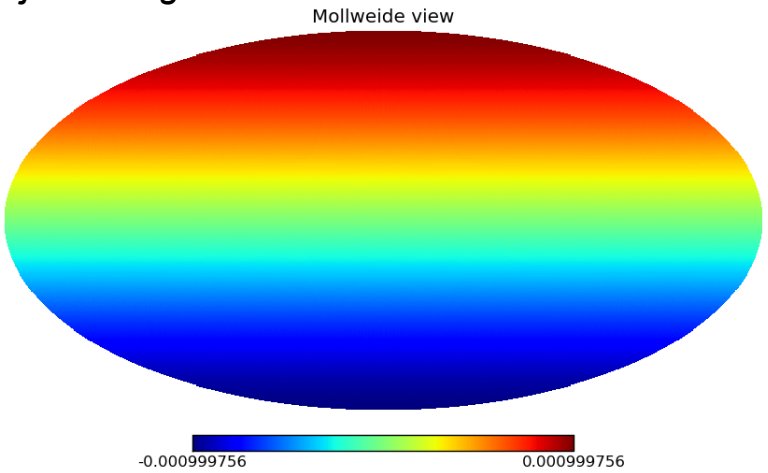

Reconstructed signal

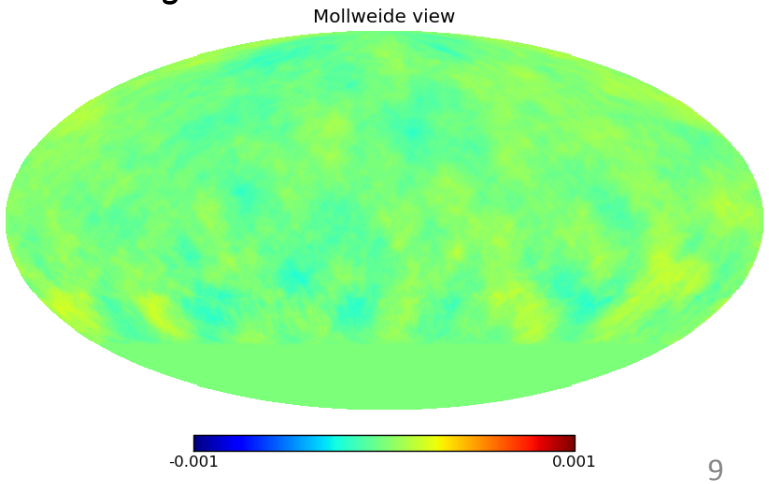

Dan Fiorino

Analysis Strategy

Mid-latitude detectors:

- Instantaneous field of view of the detector is much smaller than the 24 hr integrated field of view.

Data map (count map)

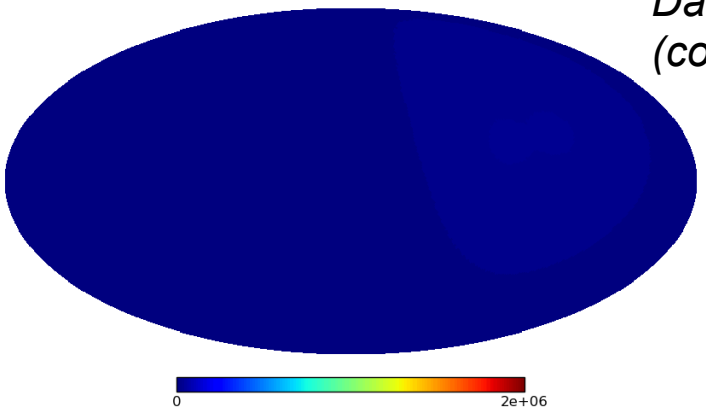

Reference map

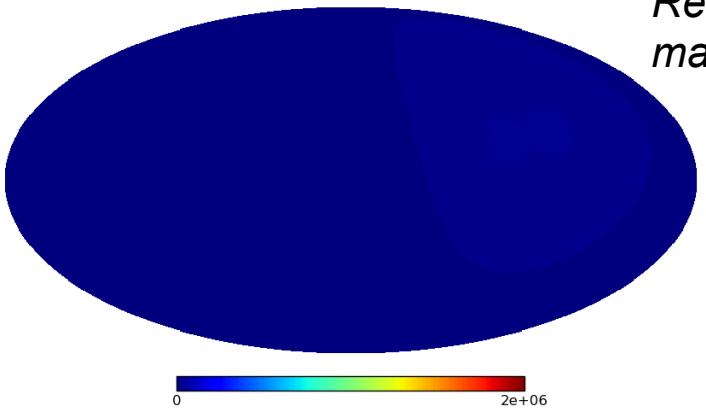

Relative intensity (or significance) map

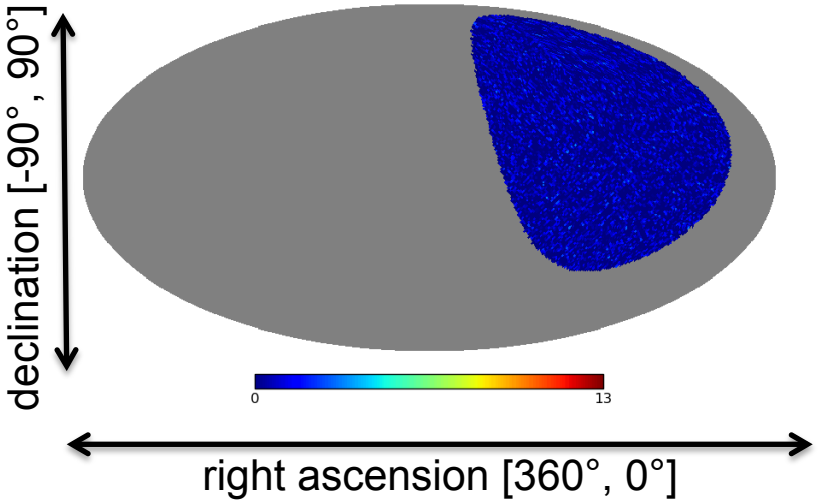

Analysis Strategy

Mid-latitude detectors:

- Instantaneous field of view of the detector is much smaller than the 24 hr integrated field of view.

Data map (count map)

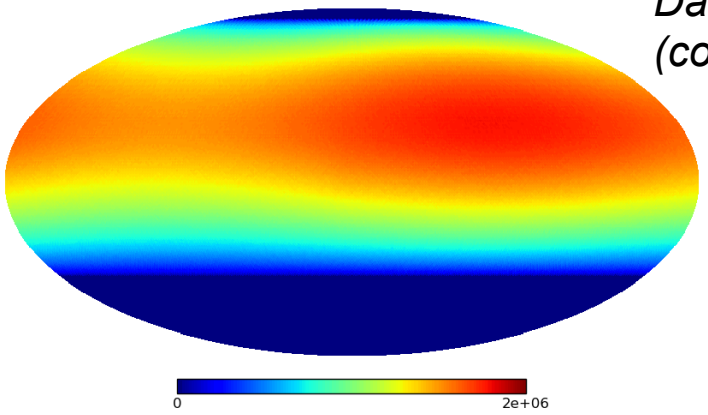

Reference map

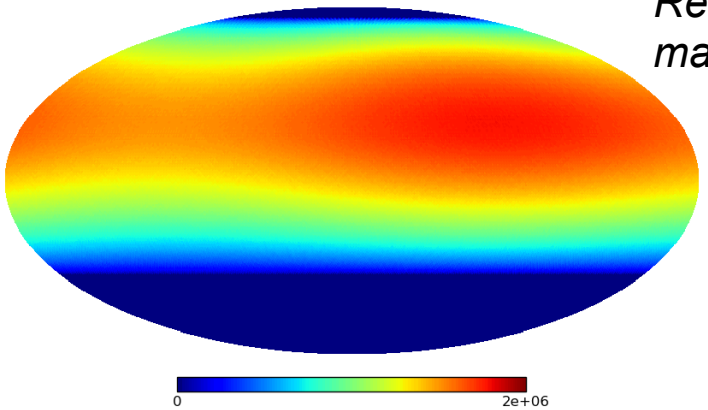

Relative intensity (or significance) map

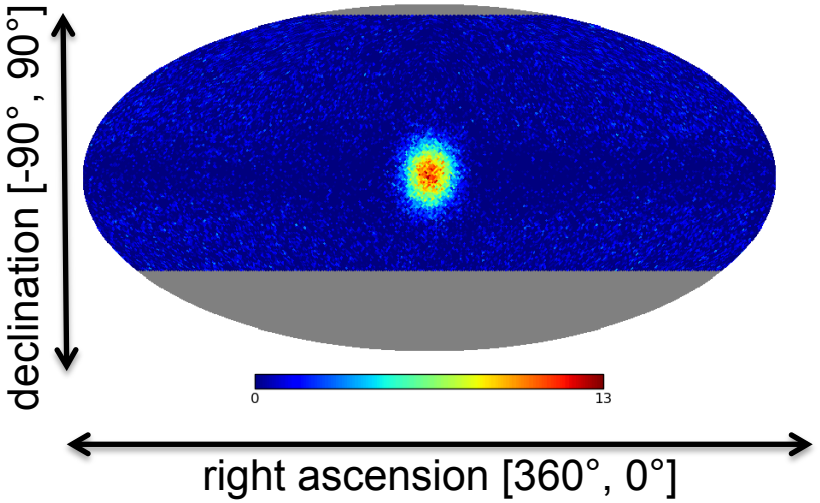

Biases of the Analysis Techniques

- Mid-latitude detectors:
  - Instantaneous exposure is smaller than the full 24 hr integrated exposure, so at any given time the detector observes only a part of the large-scale structure.
    - Large-scale structures are attenuated.
    - This effect can be mitigated by iterative methods, for example Ahlers et al., ApJ 823 (2016) 10
      - Iterative maximum likelihood method, simultaneously fits anisotropy and detector acceptance.
      - Reconstructed background expectation is re-adjusted in each iteration (iteration 1 correspond to the direct integration or time scrambling method).
      - Other iterative methods:

Cui & Ya, ICRC 2003, 2315
Tibet ASγ, ApJ 633 (2005) 1005
ARGO-YBJ, ApJ 809 (2015) 90

Maximum Likelihood Iteration

- Simulated cosmic-ray anisotropy, with the instantaneous field of view of the HAWC Observatory (19° N) at a local sidereal time of 9 hr.
- Note that at this time, the detector observes a part of the sky with a deficit, so the initial estimate for the isotropic background level (and therefore also the estimate for the amplitude of the large-scale structure) is too low.
- The iteration compensates for this effect (typically within 10 iterations).

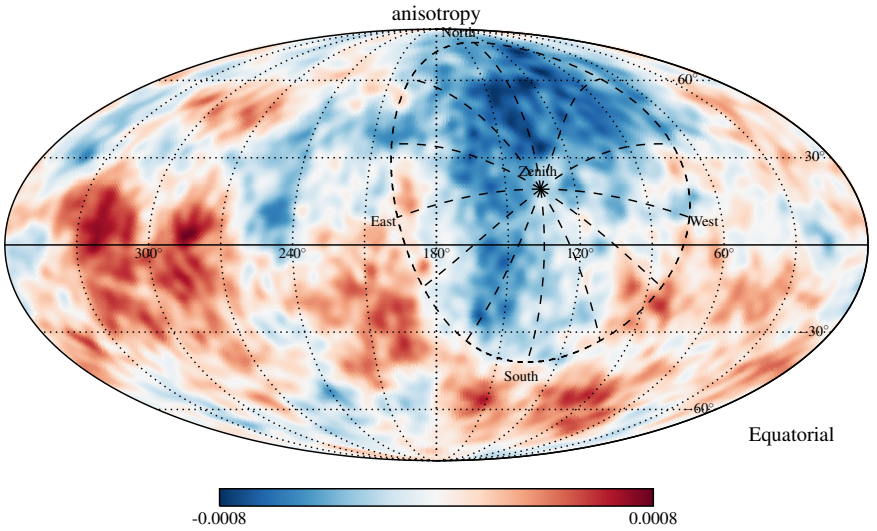

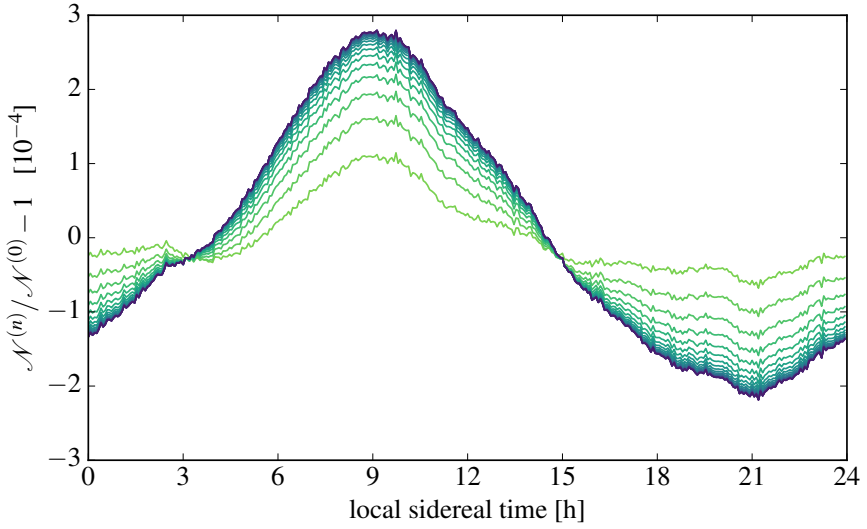

Ahlers et al., ApJ 823 (2016) 10

Systematic Biases – Summary

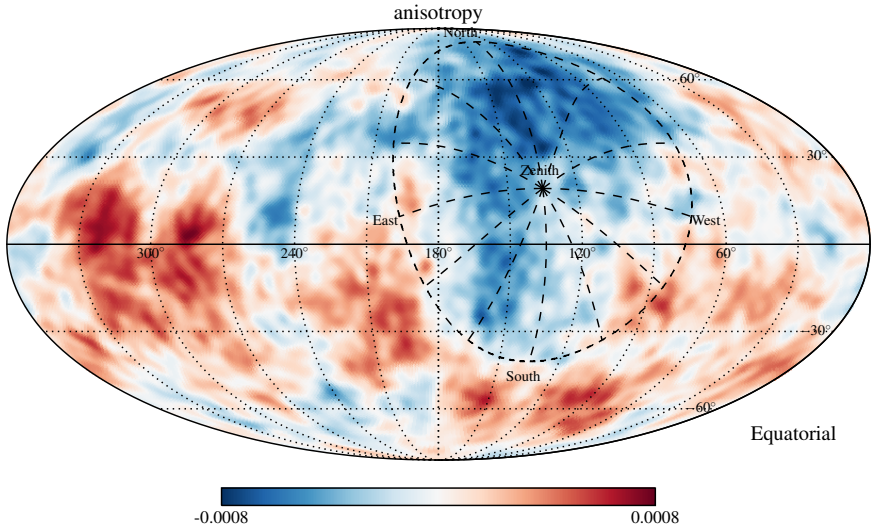

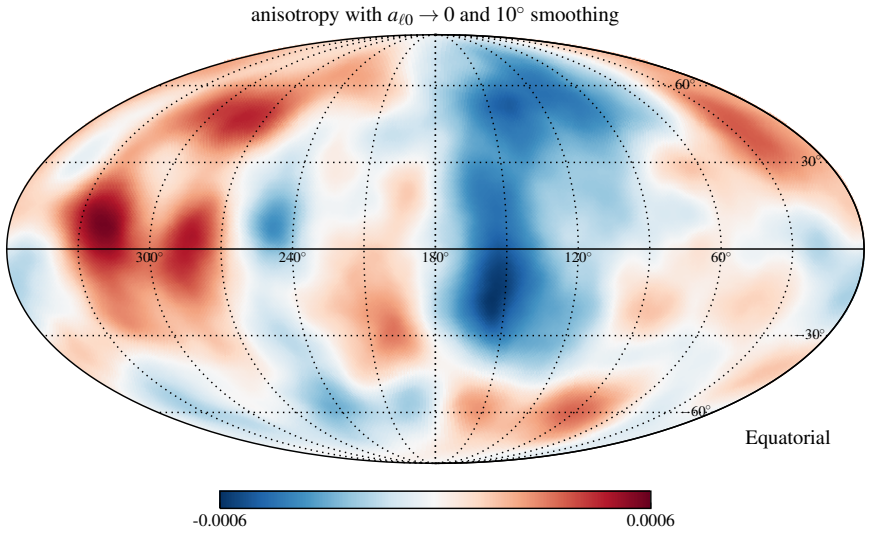

Projection and smoothing (10°)

Ahlers et al., ApJ 823 (2016) 10

Systematic Biases – Summary

1 iteration
(direct integration,
time scrambling)

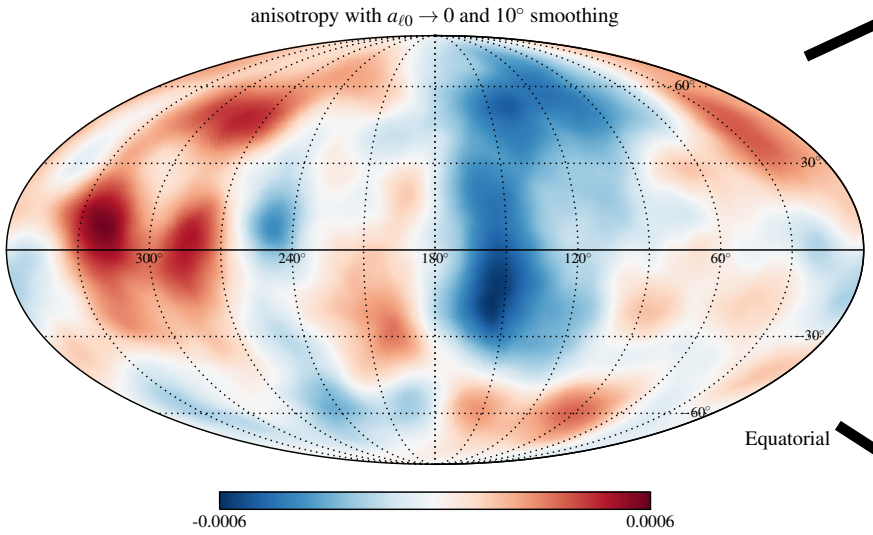

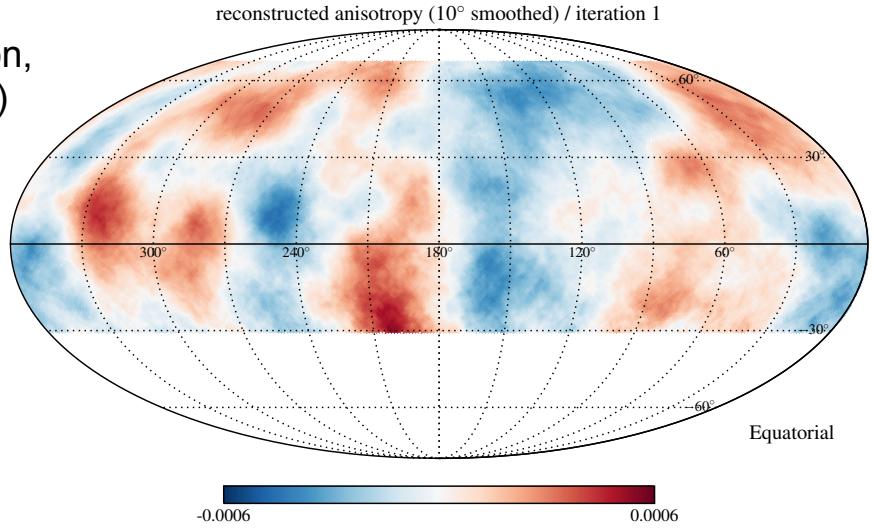

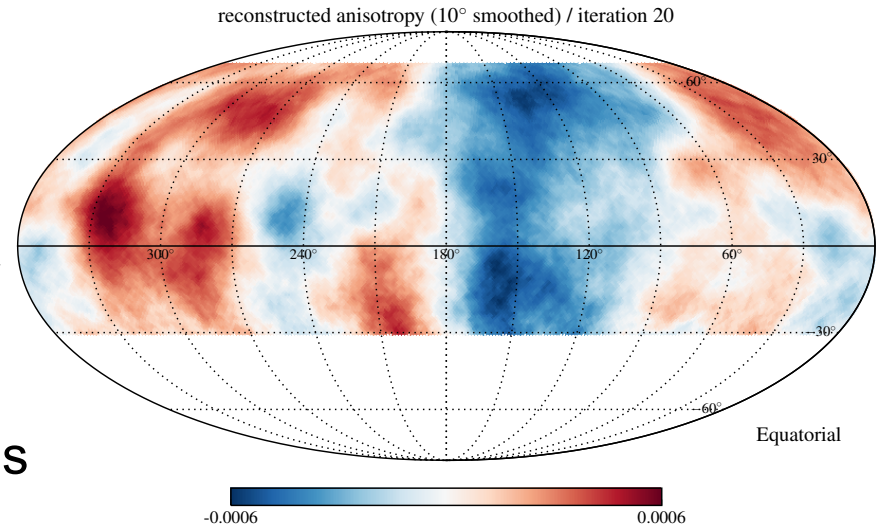

20 iterations

Ahlers et al., ApJ 823 (2016) 10

Systematic Biases – Summary

1 iteration
(direct integration,
time scrambling)

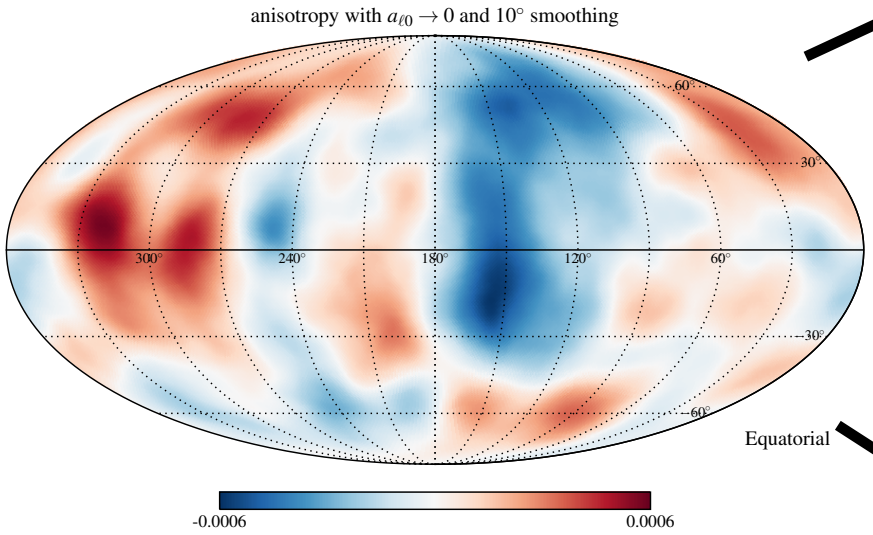

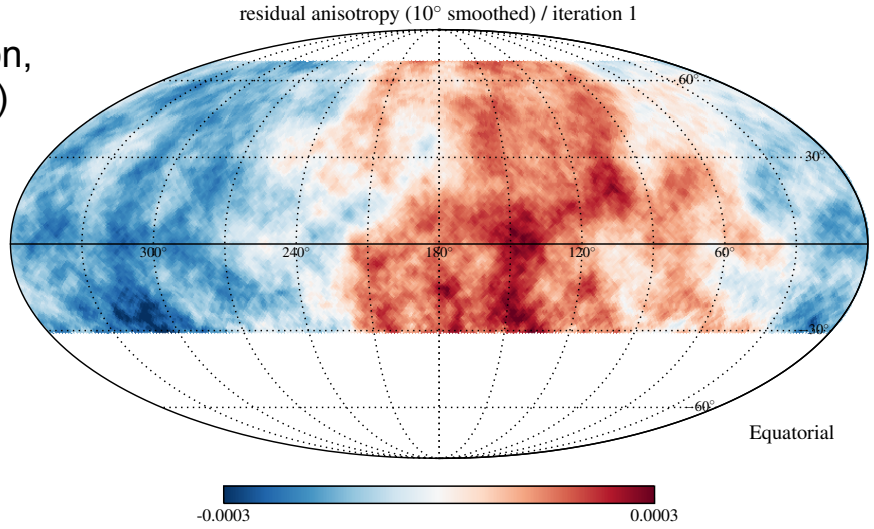

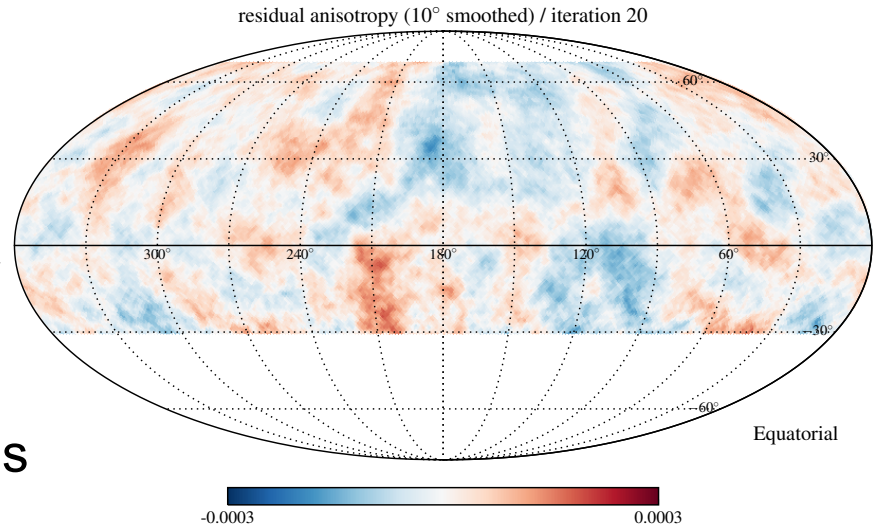

20 iterations

Ahlers et al., ApJ 823 (2016) 10

Example: HAWC

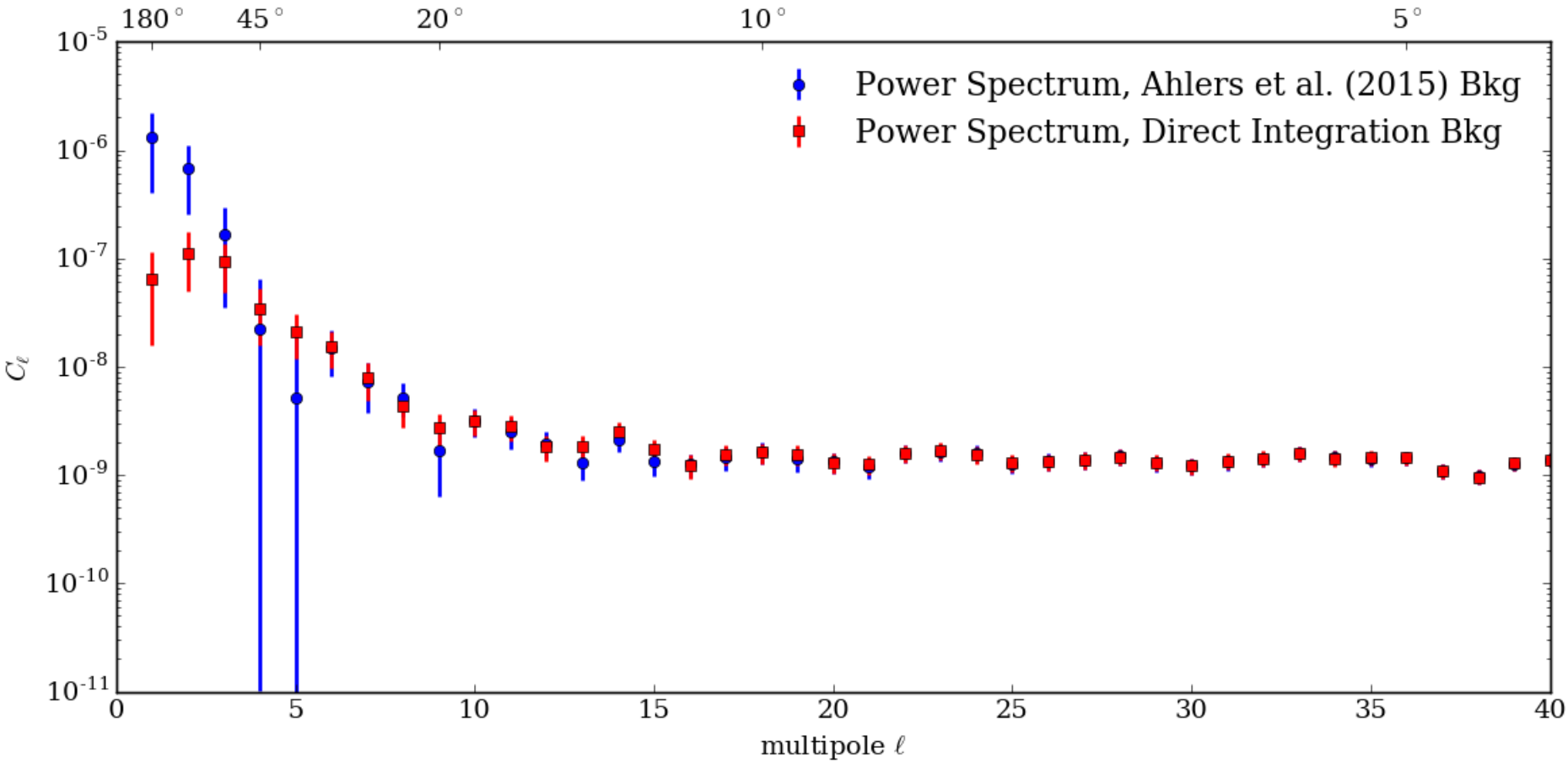

What We Know

- Relative intensity ~10^{-3} (large scale) to ~10^{-5} (medium to small scale).

ApJ 626 (2005) L29 Tibet ASγ
Science 314 (2006) 439 Tibet ASγ
PRD 75 (2007) 062003 SuperK
PRL 101 (2008) 221101 Milagro
ApJ 698 (2009) 2121 Milagro
ApJ 692 (2009) L130 EAS-TOP
ApJ 740 (2011) 16 IceCube
ApJ 765 (2013) 55 IceTop
PRD 88 (2013) 082001 ARGO-YBJ
ApJ 796 (2014) 108 HAWC
ApJ 809 (2015) 90 ARGO-YBJ
ApJ 826 (2016) 220 IceCube

- Anisotropy has a complex morphology and is not well-described by a simple dipole. There is structure at least down to 10°.

- Anisotropy is energy-dependent…
  - Large-scale structure shows phase shift above 100 TeV.
  - Small-scale excess regions show weak evidence for harder spectrum than isotropic cosmic-ray flux, and a possible cutoff ~10 TeV.

ApJL 692 (2009) L130
ApJ 826 (2016) 220

PRL 101 (2008) 221101
PRD 88 (2013) 082001
ApJ 796 (2014) 108

- Anisotropy is constant in time. No significant time variation has been observed at E > TeV after more than a decade of observations.

PRD 88 (2013) 082001
ApJ 809 (2015) 90
ApJ 826 (2016) 220
JGR 103 (1998) 17429
PRL 101 (2008) 221101

The Northern Hemisphere

detector	run dates	altitude	latitude	geomag. latitude	events	median energy
Tibet ASγ	Feb1997 – Nov 2005	4300 m	30.1° N	+24°	4 x 10^9	~ 3 TeV
Milagro	July 2000 – July 2007	2630 m	35.9° N	+42°	220 x 10^9	~ 1 TeV
ARGO-YBJ	Nov 2007 – May 2012	4300 m	30.1° N	+24°	220 x 10^9	~ 1 TeV
HAWC	June 2013 -	4100 m	19.0° N	+30°	*86 x 10^9*	~ 2 TeV

HAWC

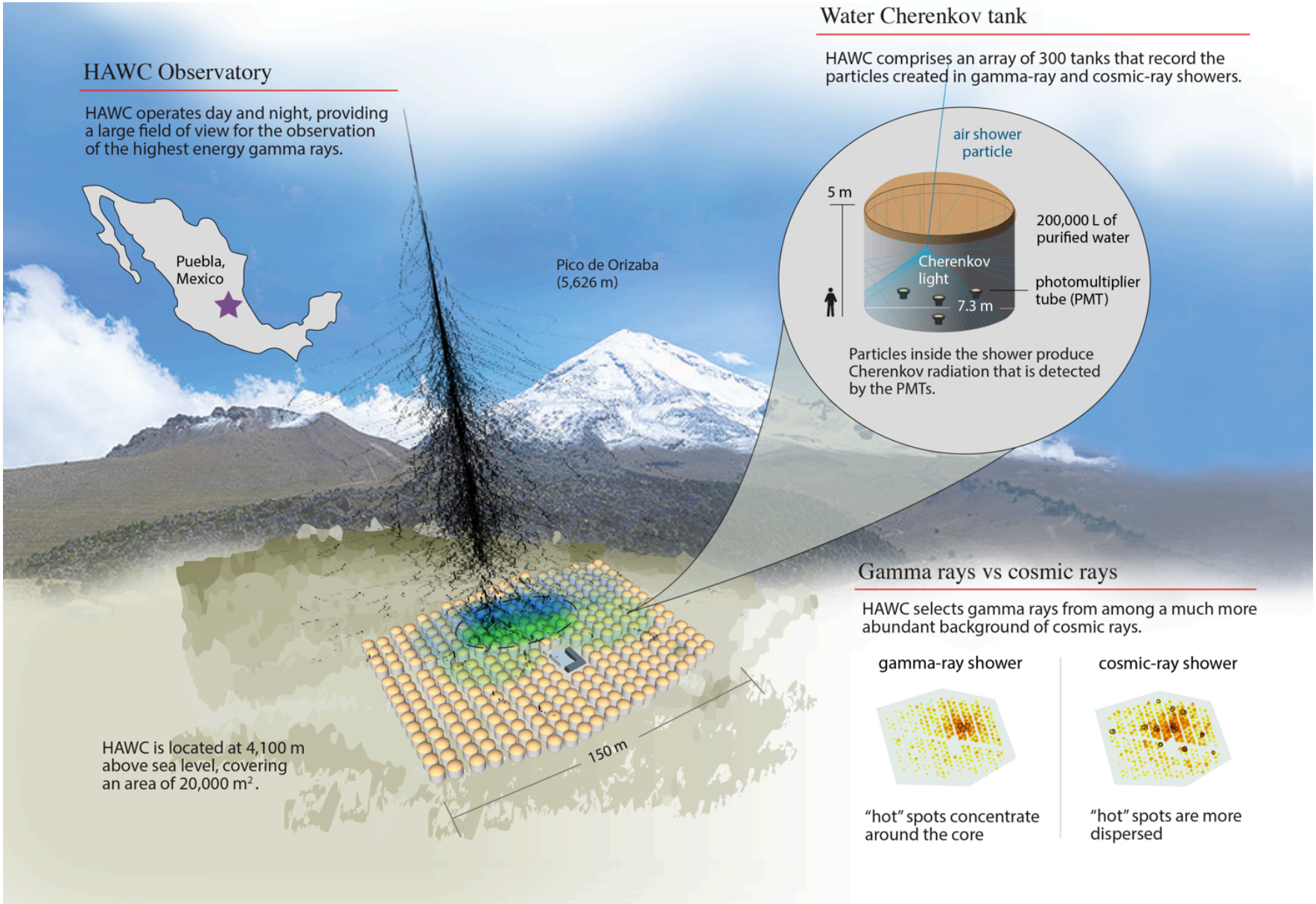
HAWC Observatory
HAWC operates day and night, providing a large field of view for the observation of the highest energy gamma rays.
Puebla, Mexico
Pico de Orizaba (5,626 m)
HAWC is located at 4,100 m above sea level, covering an area of 20,000 m².
150 m
Water Cherenkov tank
HAWC comprises an array of 300 tanks that record the particles created in gamma-ray and cosmic-ray showers.
air shower particle
5 m
200,000 L of purified water
Cherenkov light
photomultiplier tube (PMT)
7.3 m
Particles inside the shower produce Cherenkov radiation that is detected by the PMTs.
Gamma rays vs cosmic rays
HAWC selects gamma rays from among a much more abundant background of cosmic rays.
gamma-ray shower
cosmic-ray shower
"hot" spots concentrate around the core
"hot" spots are more dispersed

The Southern Hemisphere

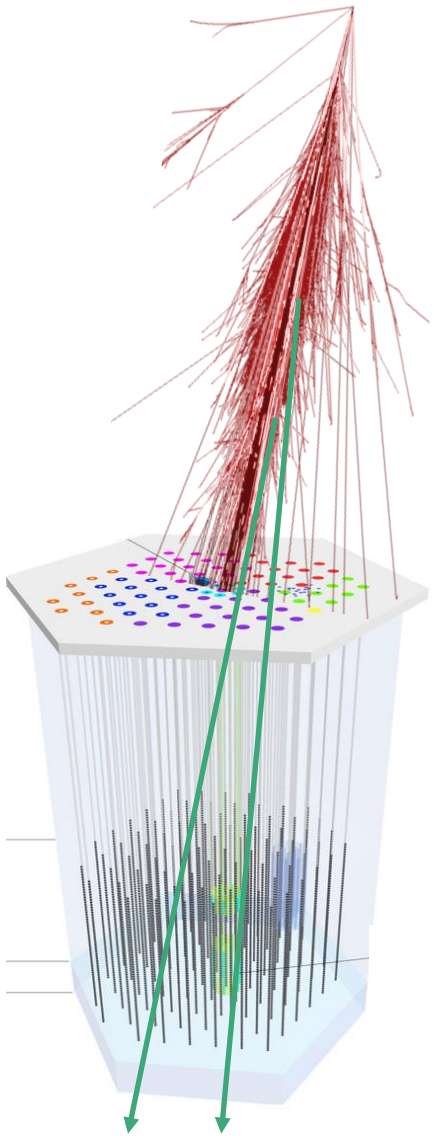

detector	run dates	altitude	events	median energy
IceCube	May 2009 –		320 x 10^9	~ 20 TeV
IceTop	May 2009 –	2835 m	0.2 x 10^9	~ 1.6 PeV

- IceCube is sensitive to down-going muons produced in cosmic-ray air showers
  - Rate: ~ 2.5 – 2.9 kHz
  - Median angular resolution 3°
- IceTop is an air shower array with a threshold of ~ 300 TeV
  - Rate: ~ 30 Hz
- Instantaneous field of view is identical to time-integrated field of view.

Large Scale Anisotropy

HAWC-100

D. Fiorino

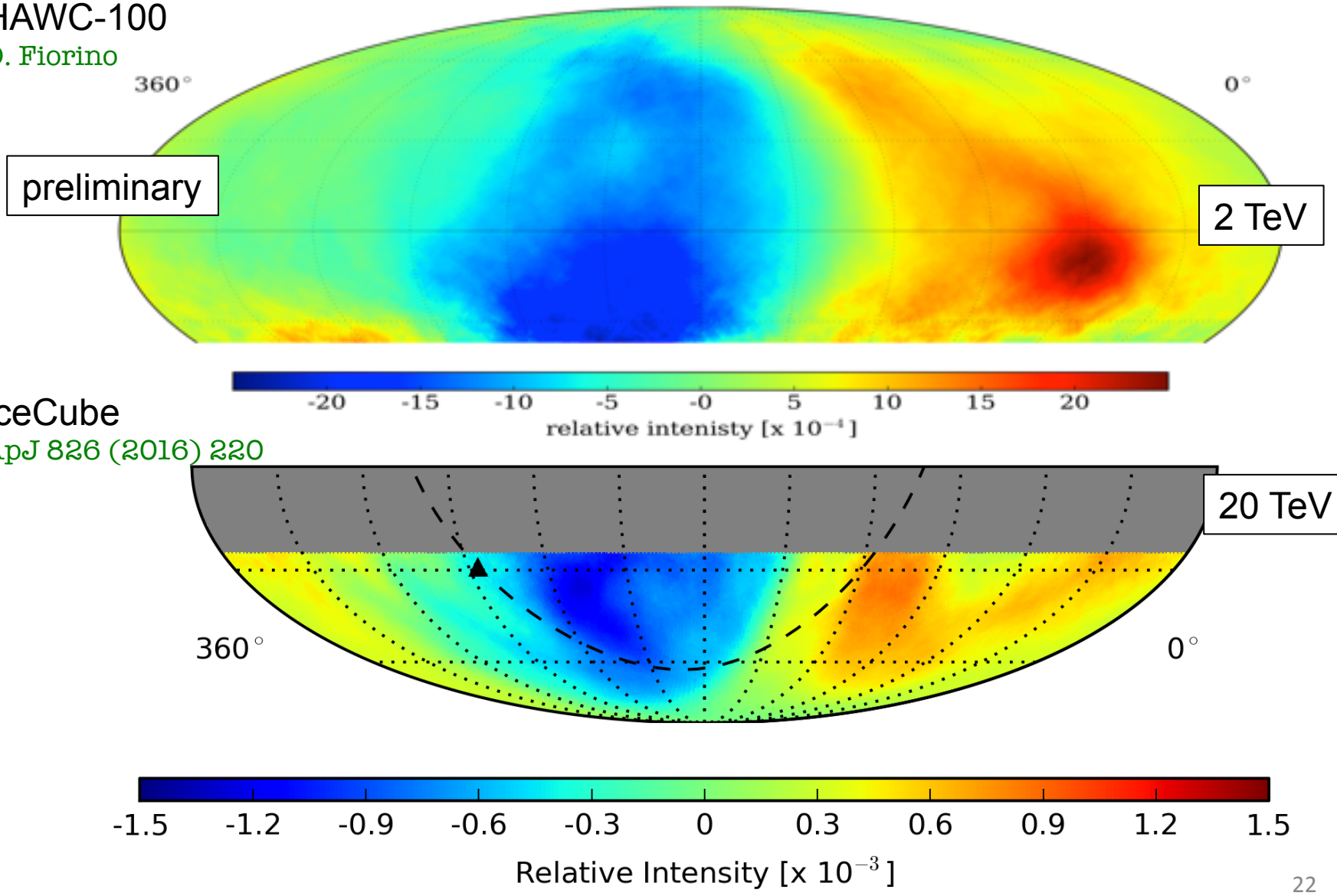

HAWC Large-Scale Anisotropy

- 241 stable sidereal days with 19 x 10^9 event (E_{med} = 6.7 TeV) – restrictive cuts for energy analysis.
- HAWC still has uneven coverage throughout the year.
- Amplitude from multipole fit A = (1.14 ± 0.94) x 10^{-3}

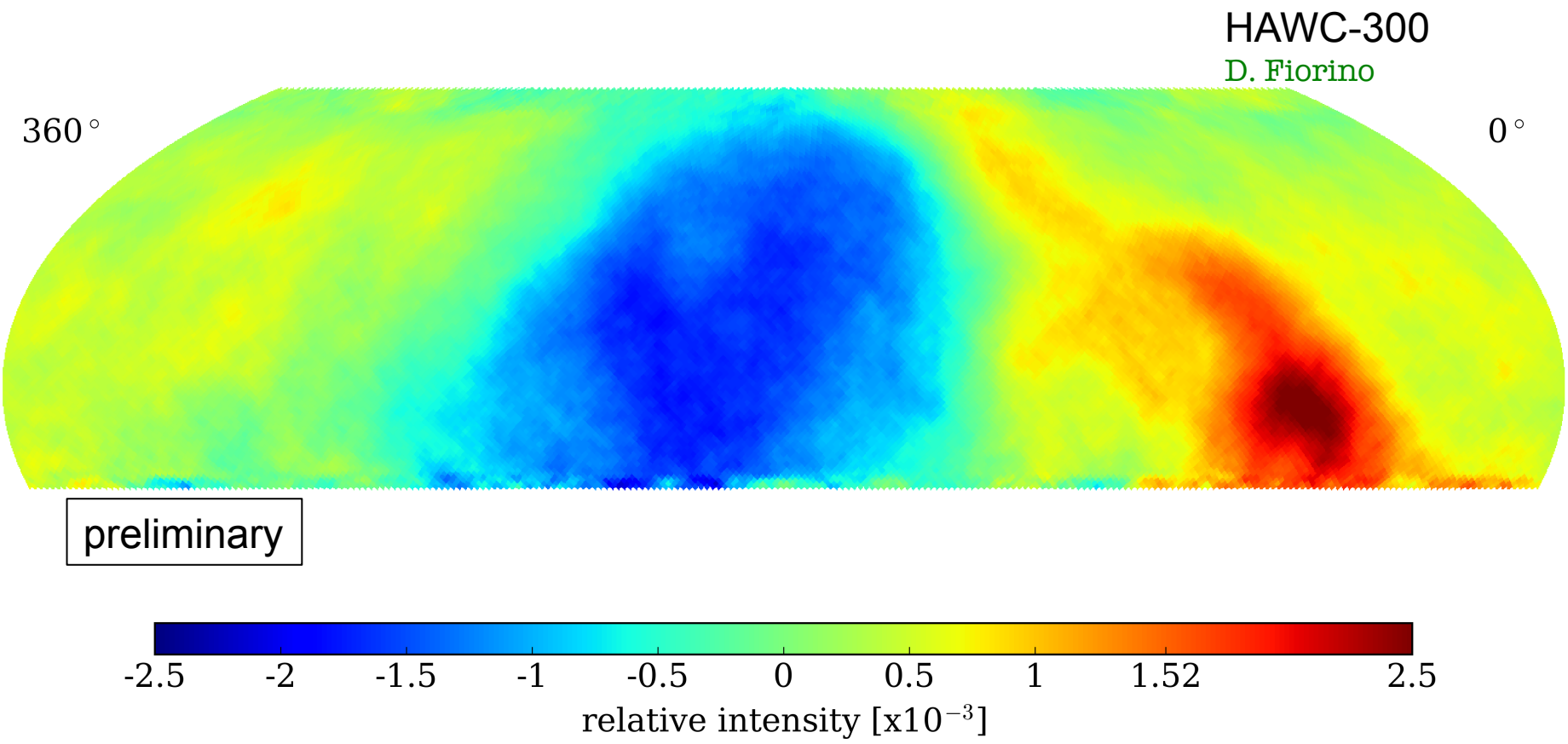

Energy/Scale Matching

- The combined HAWC and IceCube sky maps at 13 TeV median energy on the same relative intensity scale show a stronger amplitude in the North.
- Energy matching is difficult because of the poor energy resolution of the IceCube muon-based data set (0.5 in log(*E*/[GeV])).
- Energy matching is important because the anisotropy is strongly energy-dependent.

HAWC-300
D. Fiorino

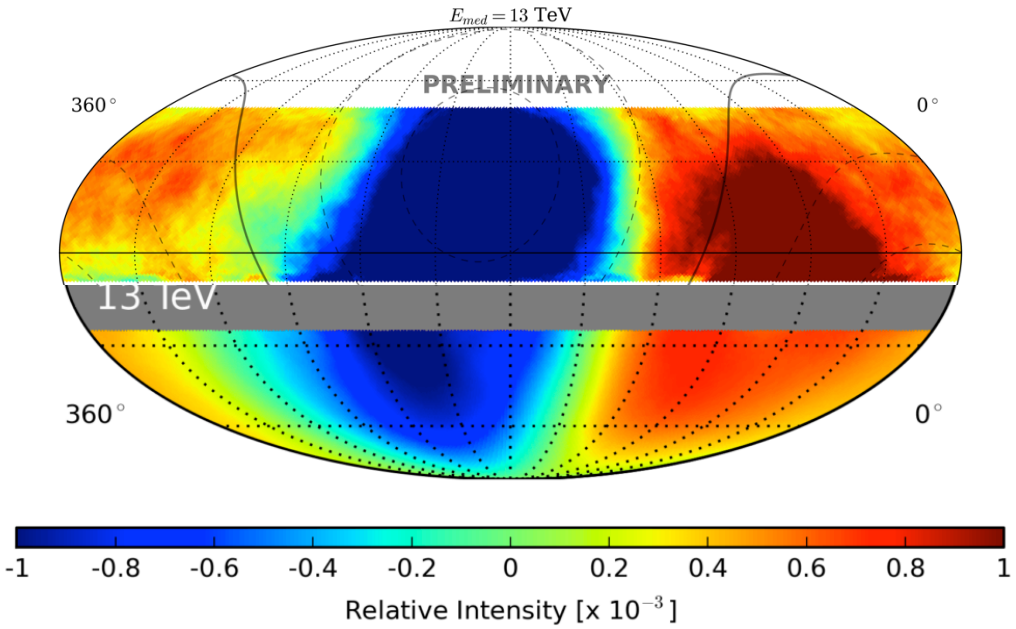

IceCube
ApJ 826 (2016) 220

Energy Dependence in IceCube

- Data is split into nine energy bands with median energy from 13 TeV to 5.3 PeV based on the number of PMTs with signal and zenith angle.
- Energy distributions of the bins have considerable overlap due to the limited energy resolution of IceCube for cosmic rays.

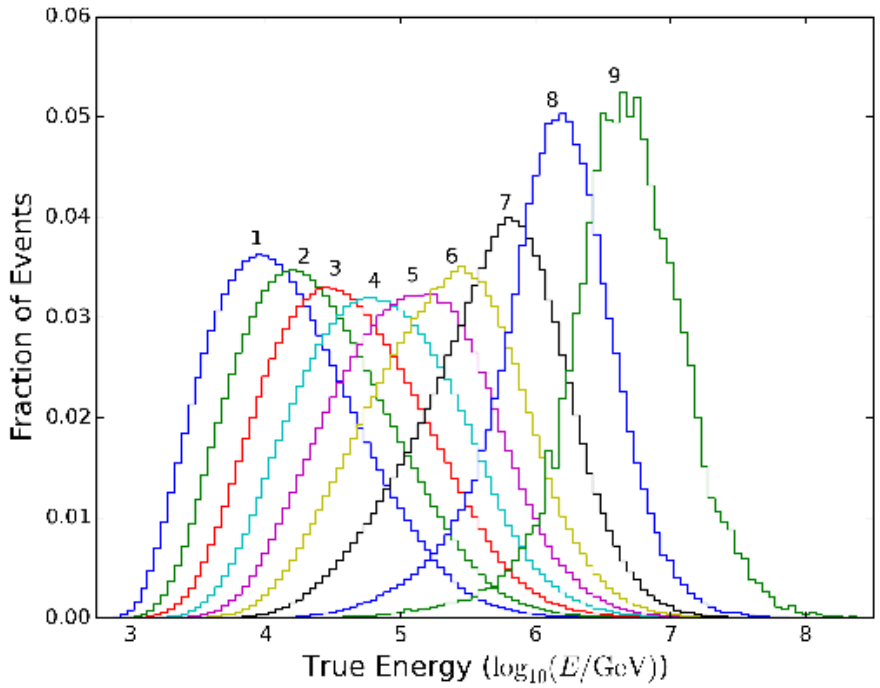

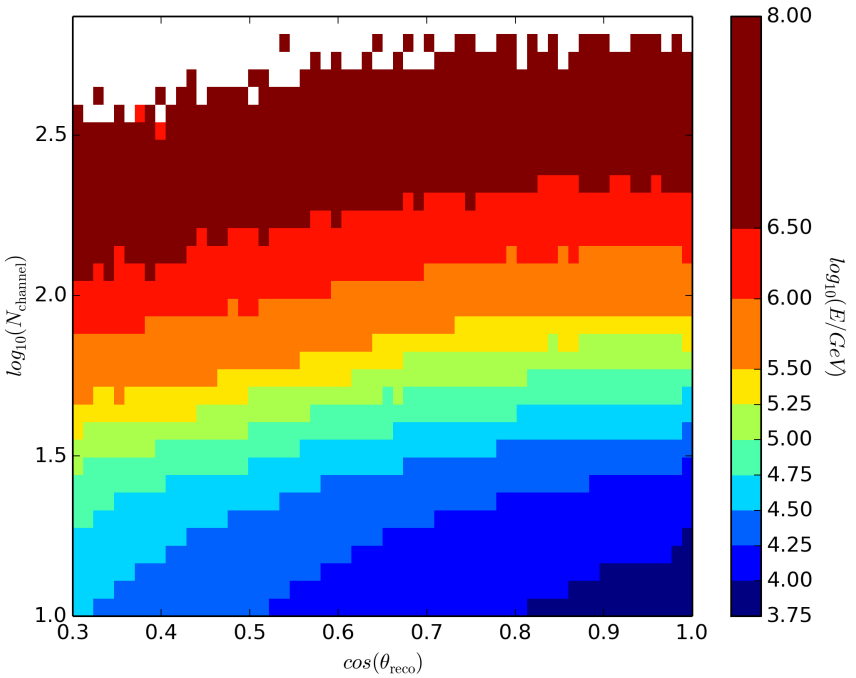

IceCube Collab.,
ApJ 826 (2016) 220

Energy Dependence

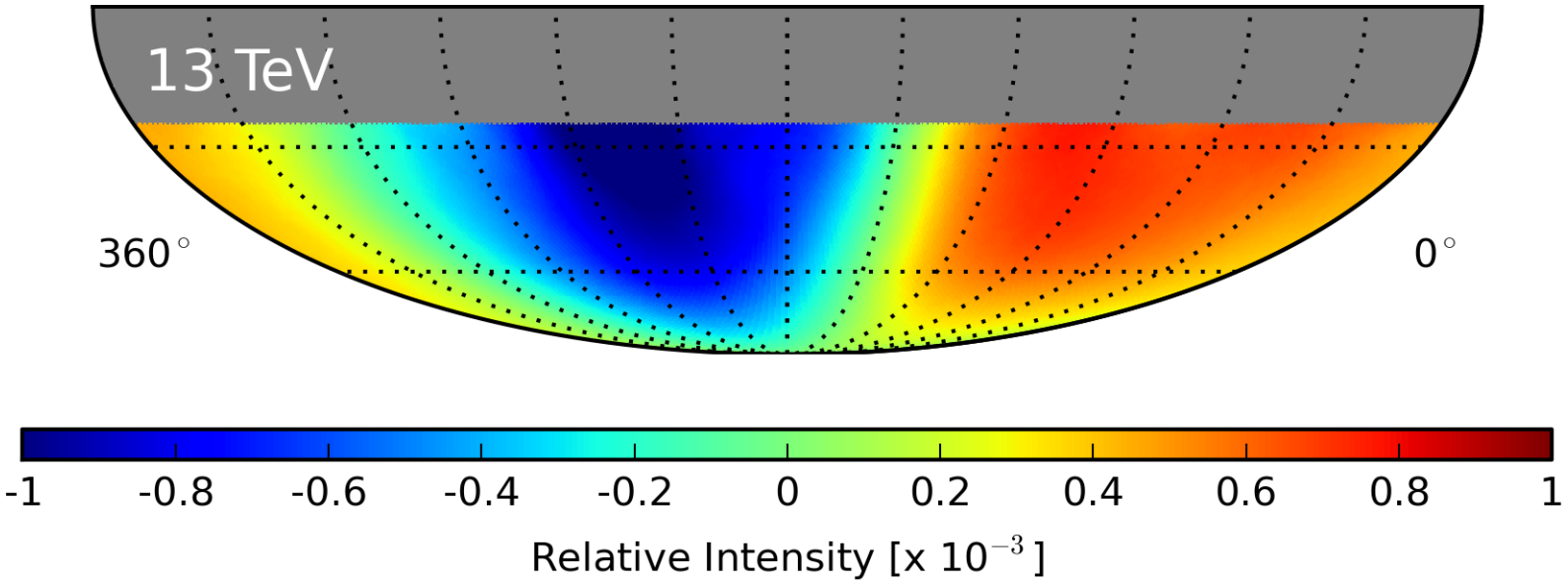

Energy Dependence

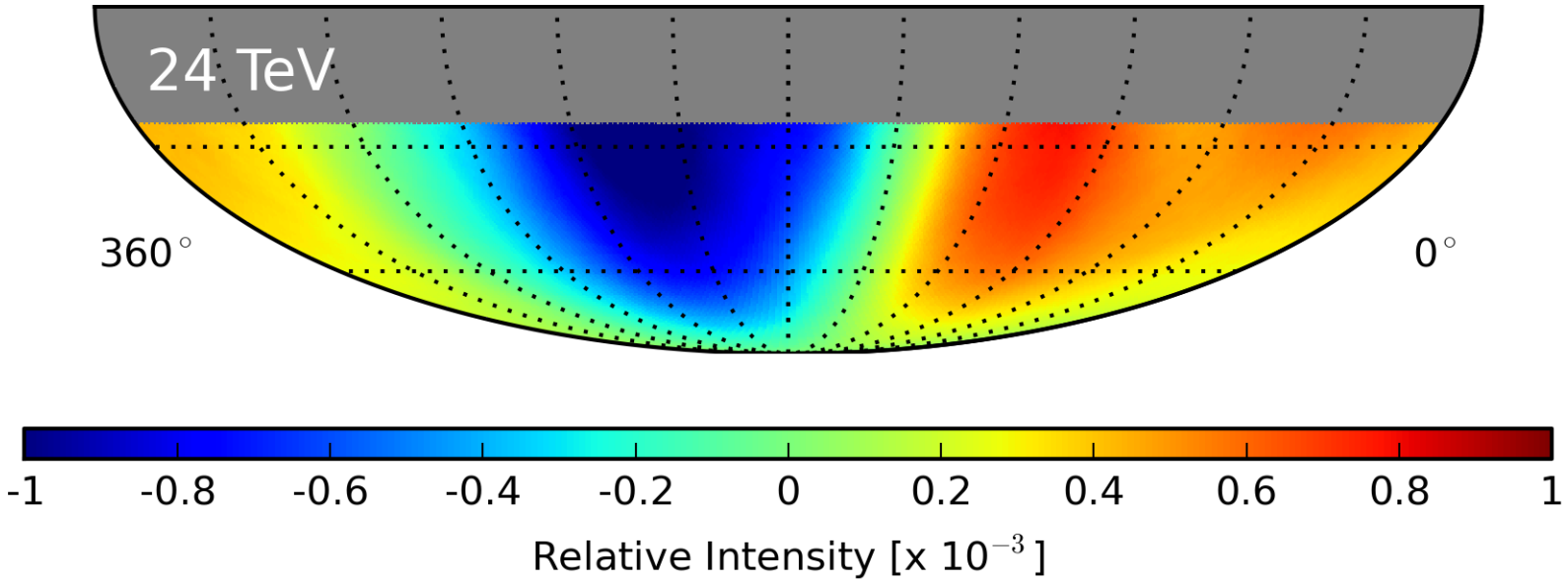

Energy Dependence

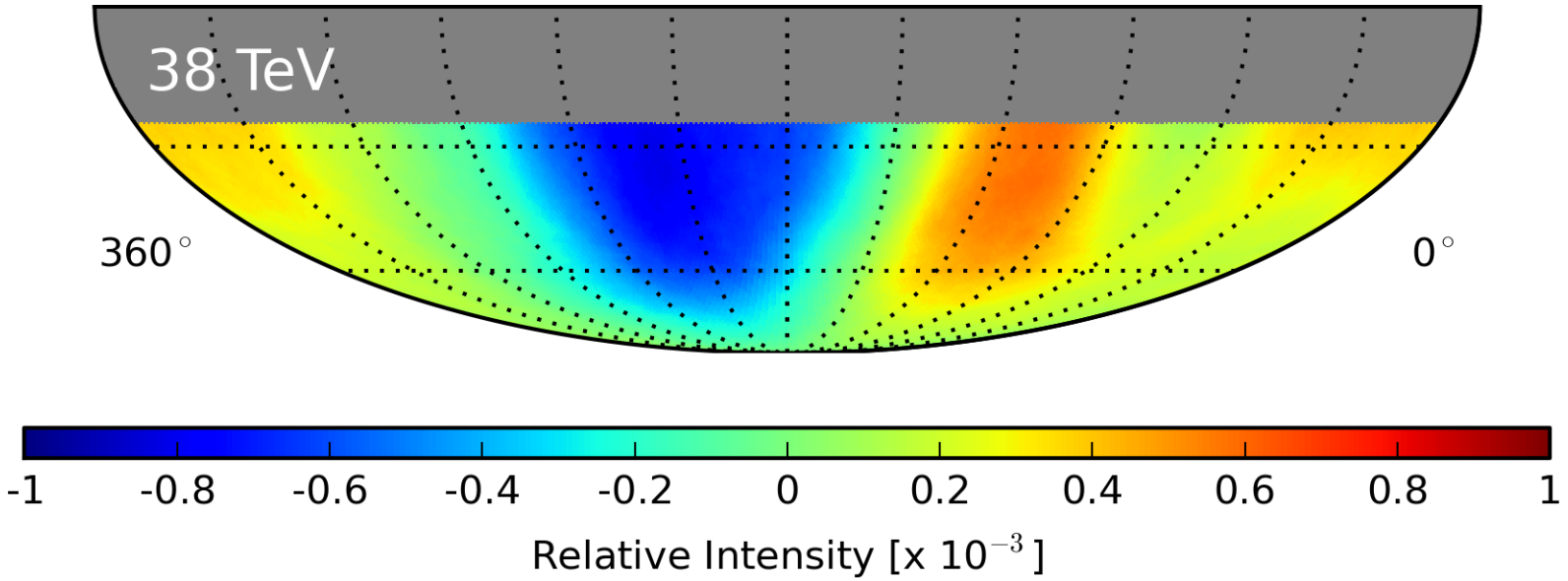

Energy Dependence

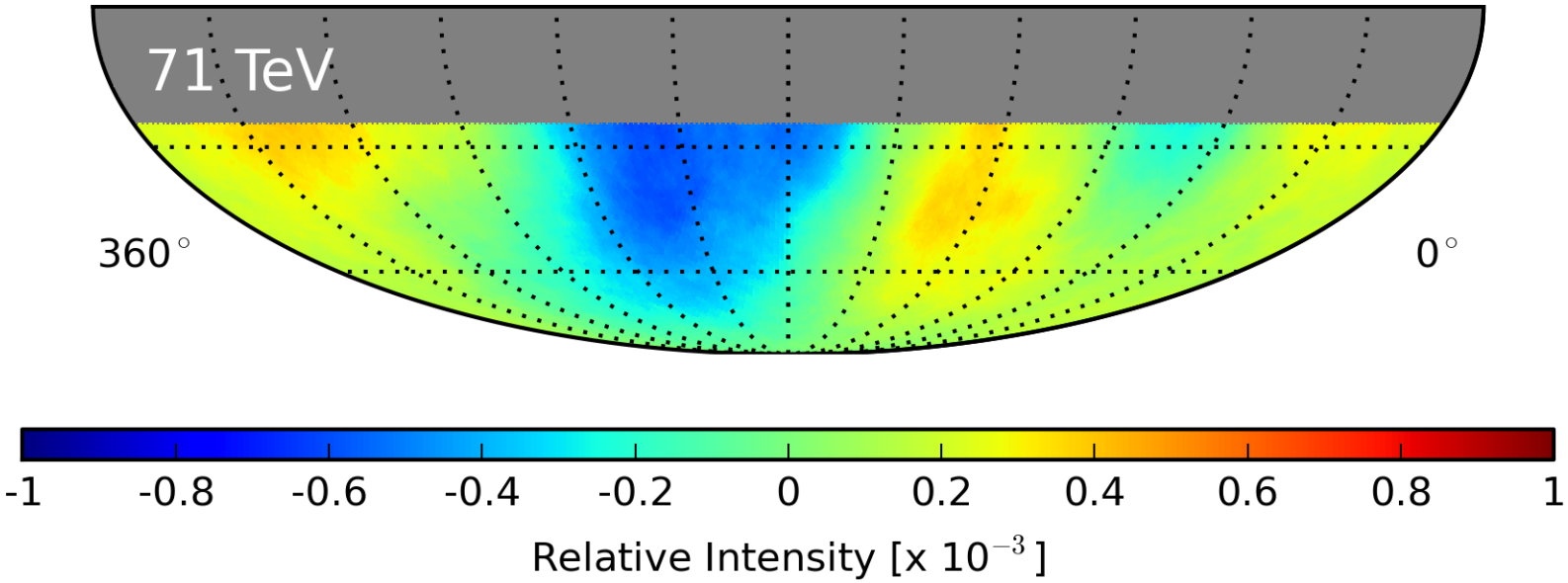

Energy Dependence

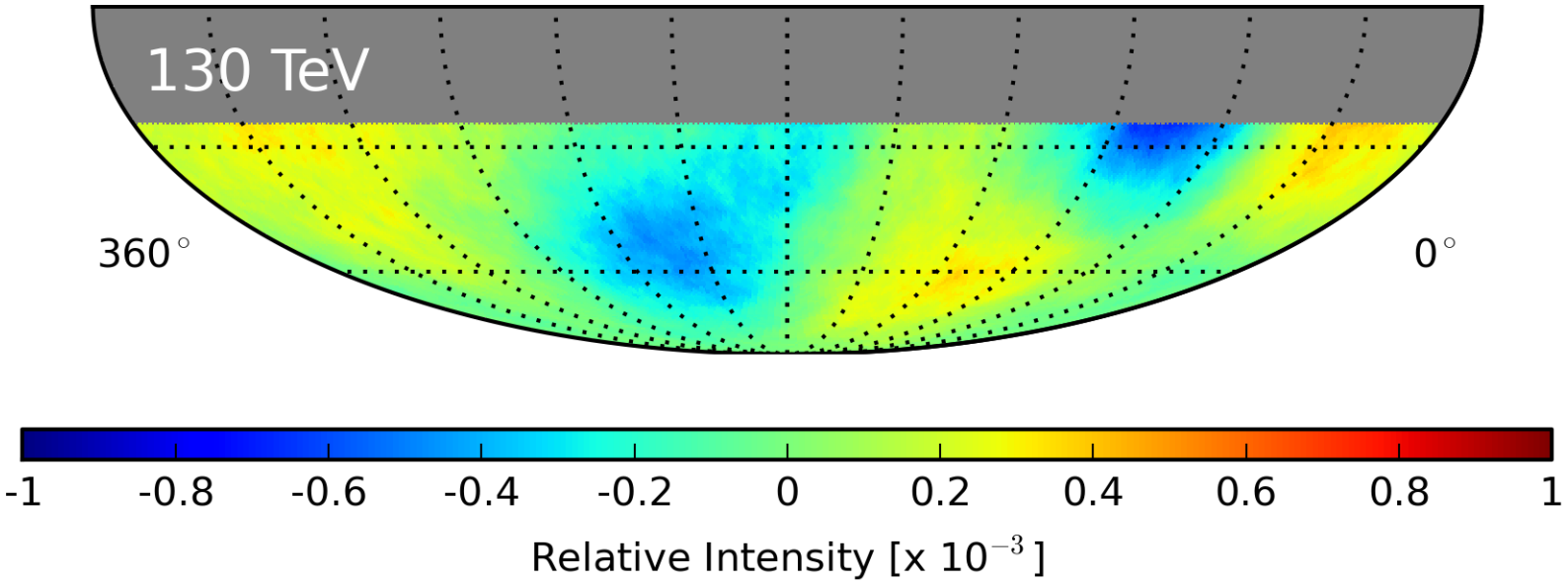

Energy Dependence

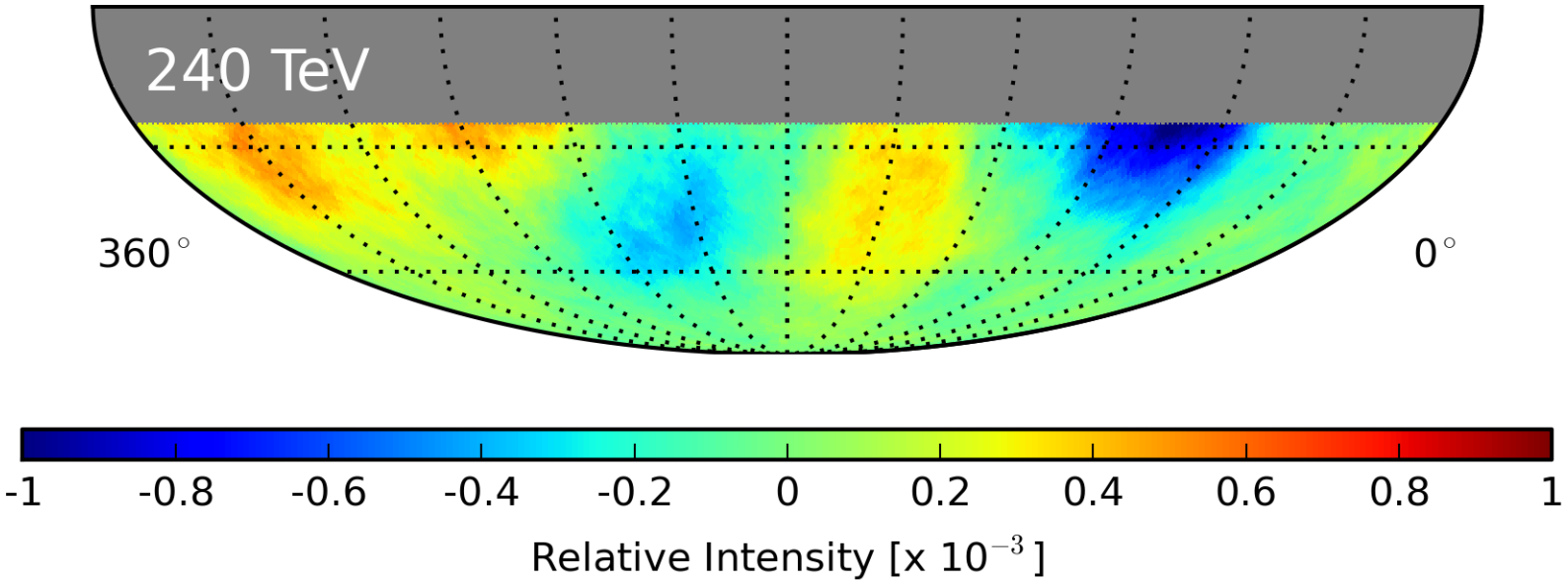

Energy Dependence

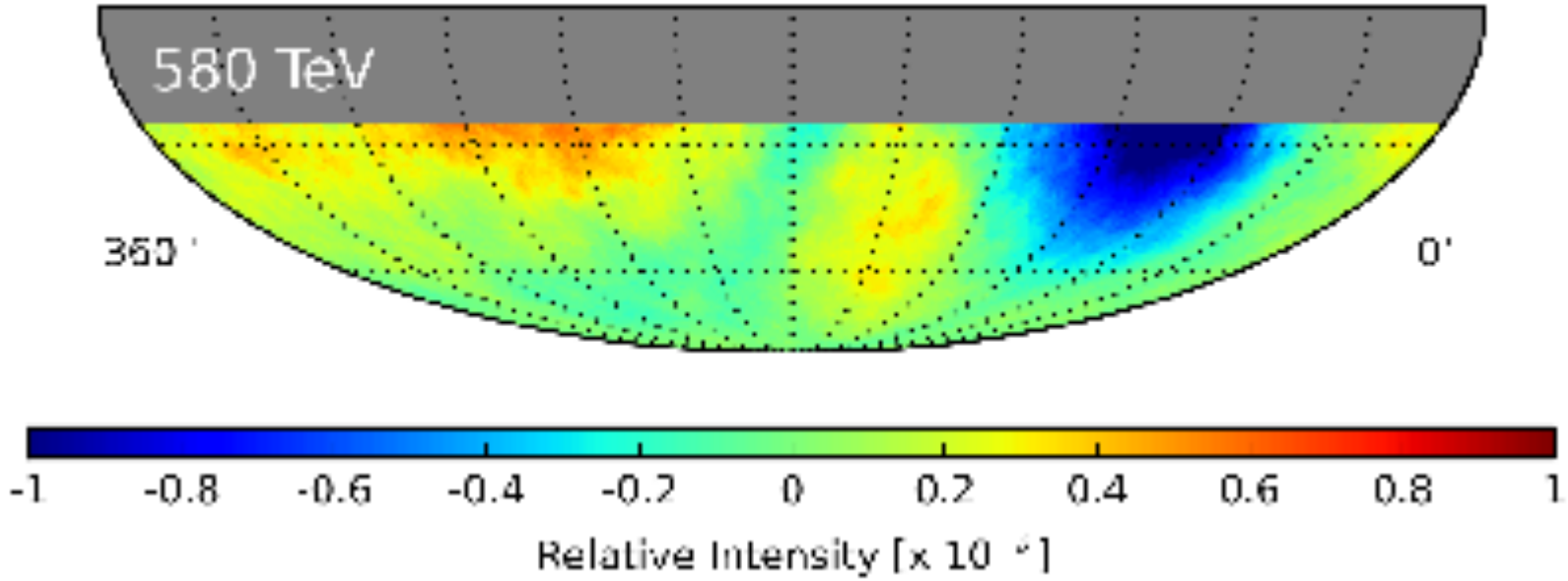

Energy Dependence

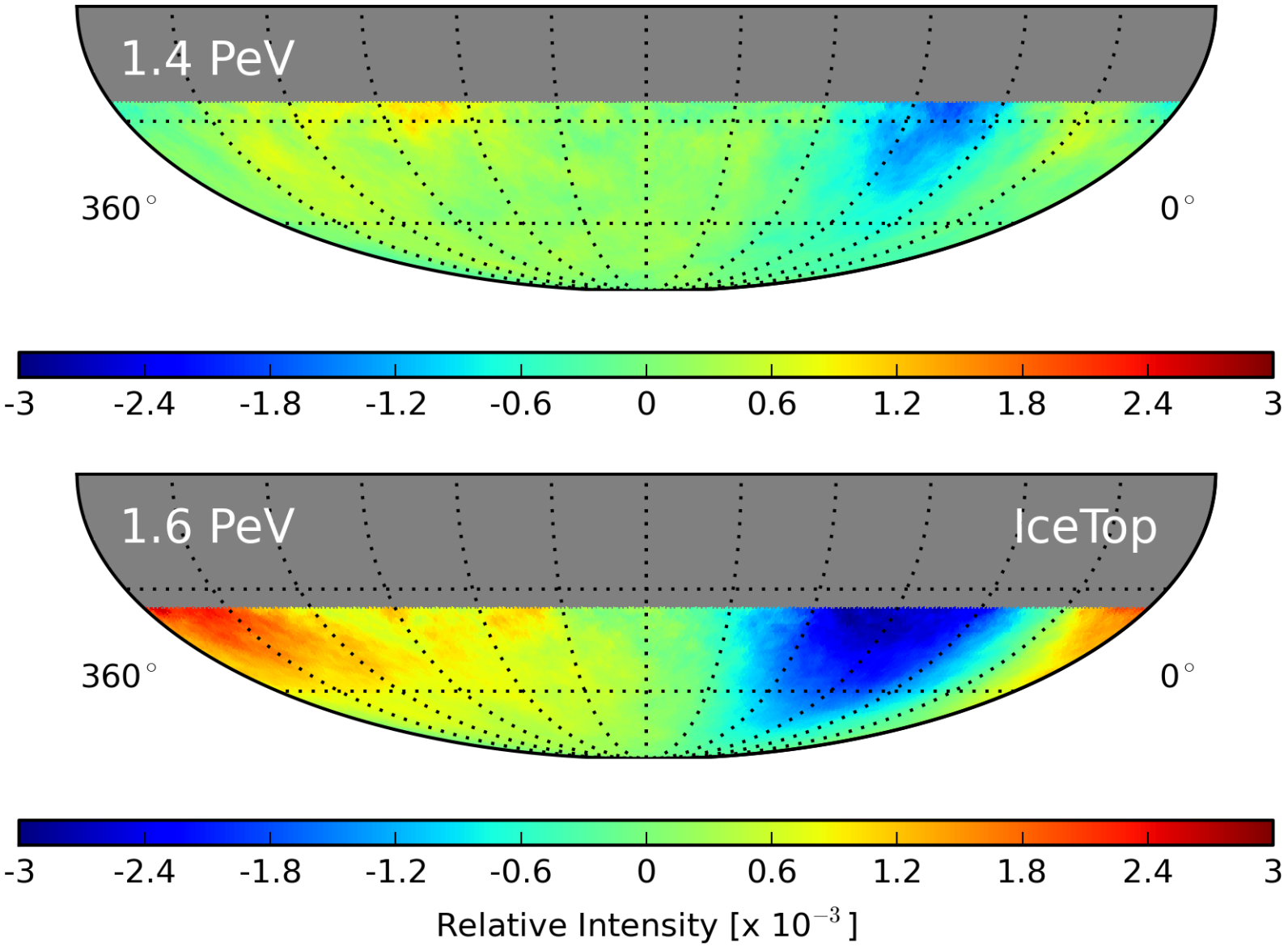

Energy Dependence

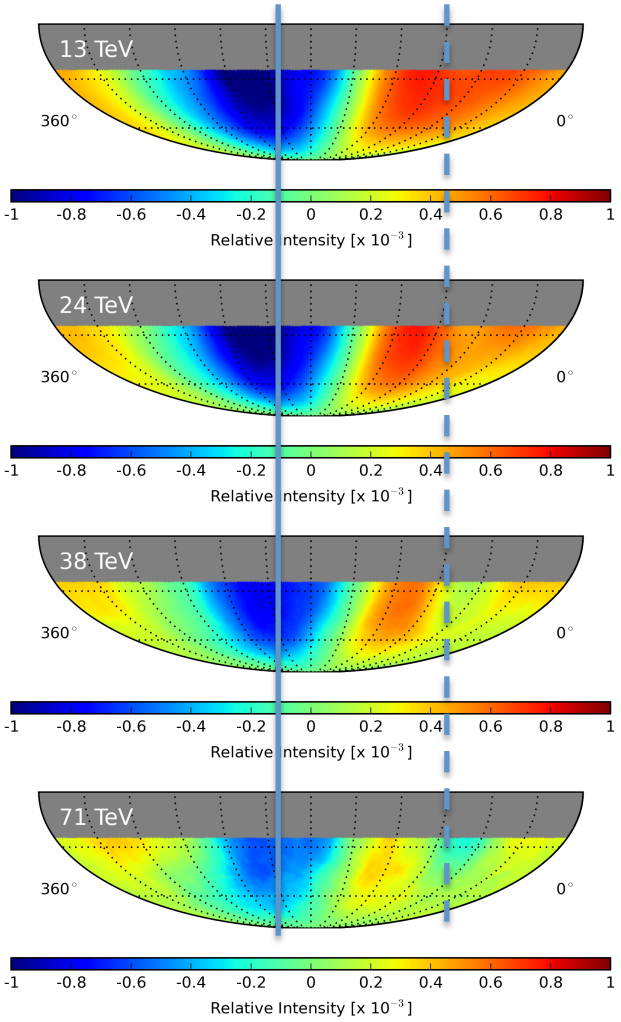

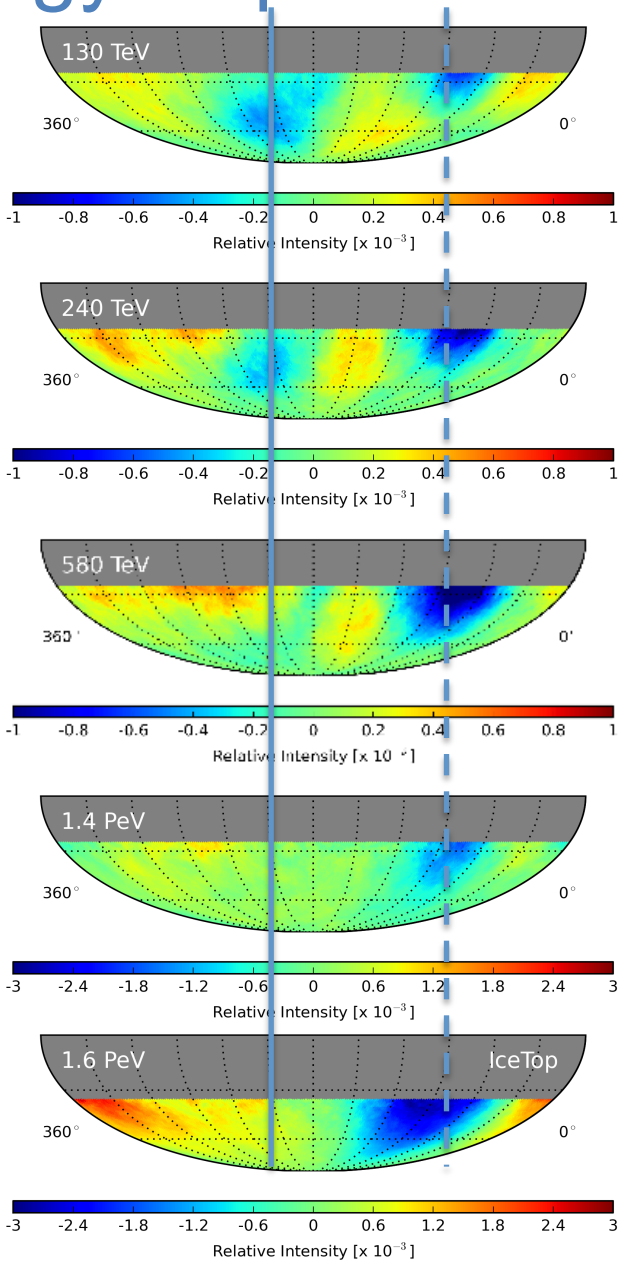

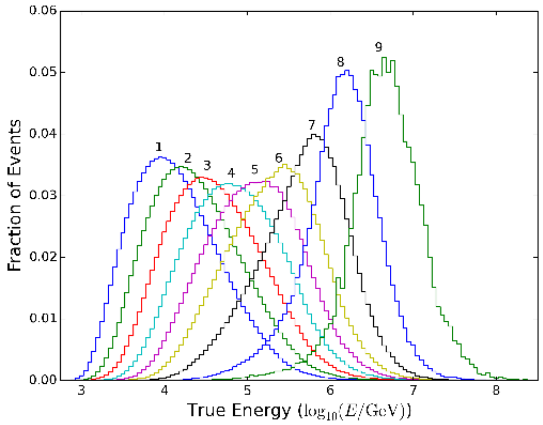

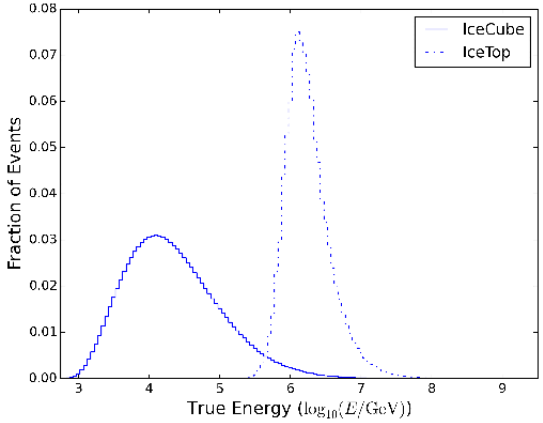

IceCube Collab.,
ApJ 826 (2016) 220

Energy Dependence

- IceCube data show an abrupt phase change of the (large-scale) anisotropy above 100 TeV.
- Plots show dipole component of fit to the full harmonic series.

IceCube
IceTop

Dipole amplitude

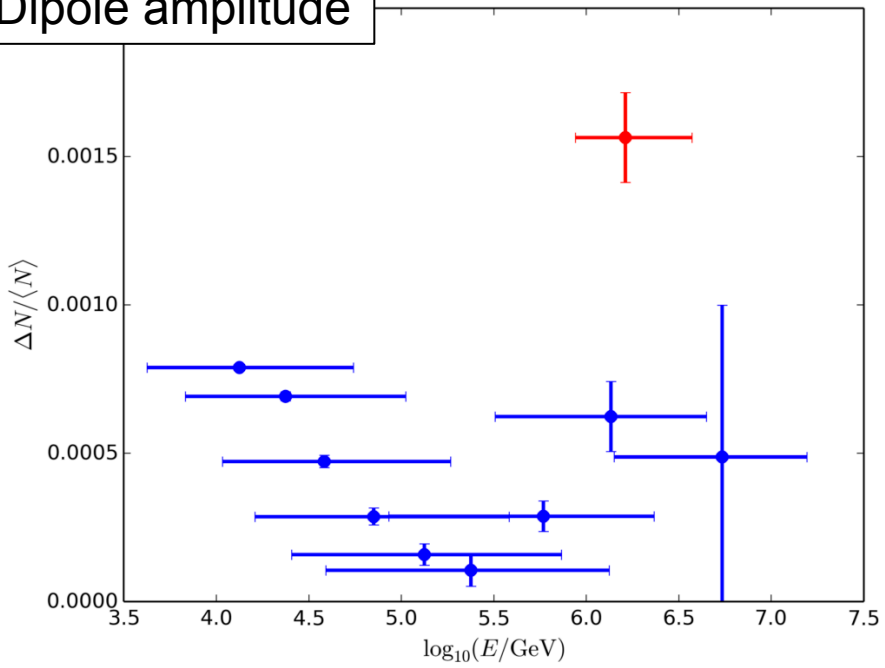

Dipole phase

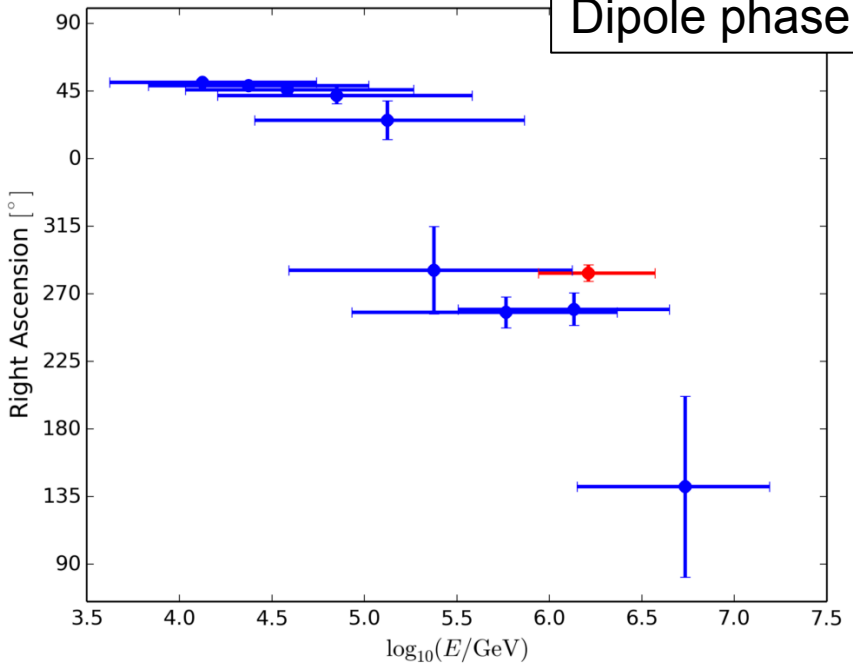

IceCube Collab.,
ApJ 826 (2016) 220

Energy Dependence

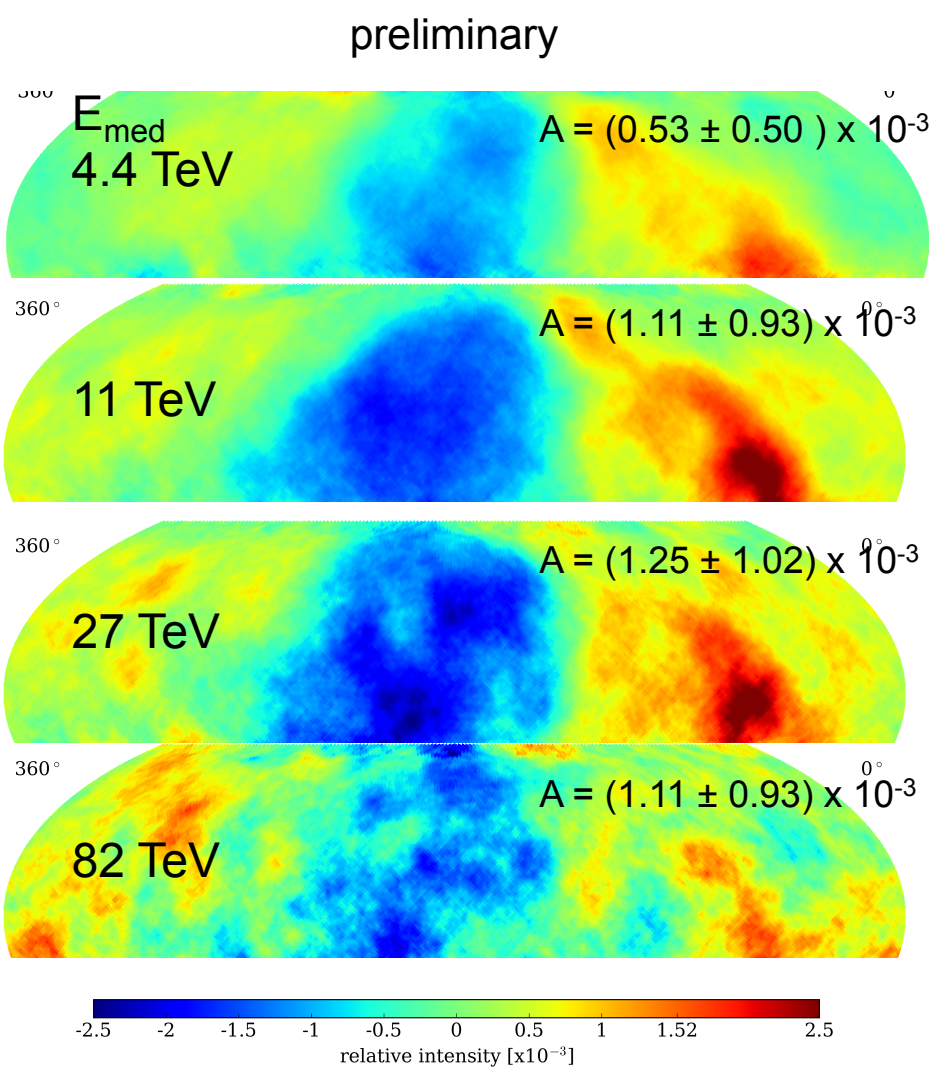

HAWC-300

D. Fiorino

- 241 days of HAWC, 19 billion events.
- Sky maps shown after 10° top-hat smoothing.
- The amplitudes are the dipole moment of a full multipole fit (note large error bars).
- Fluctuations take over at E_{med} = 82 TeV.

Energy Dependence

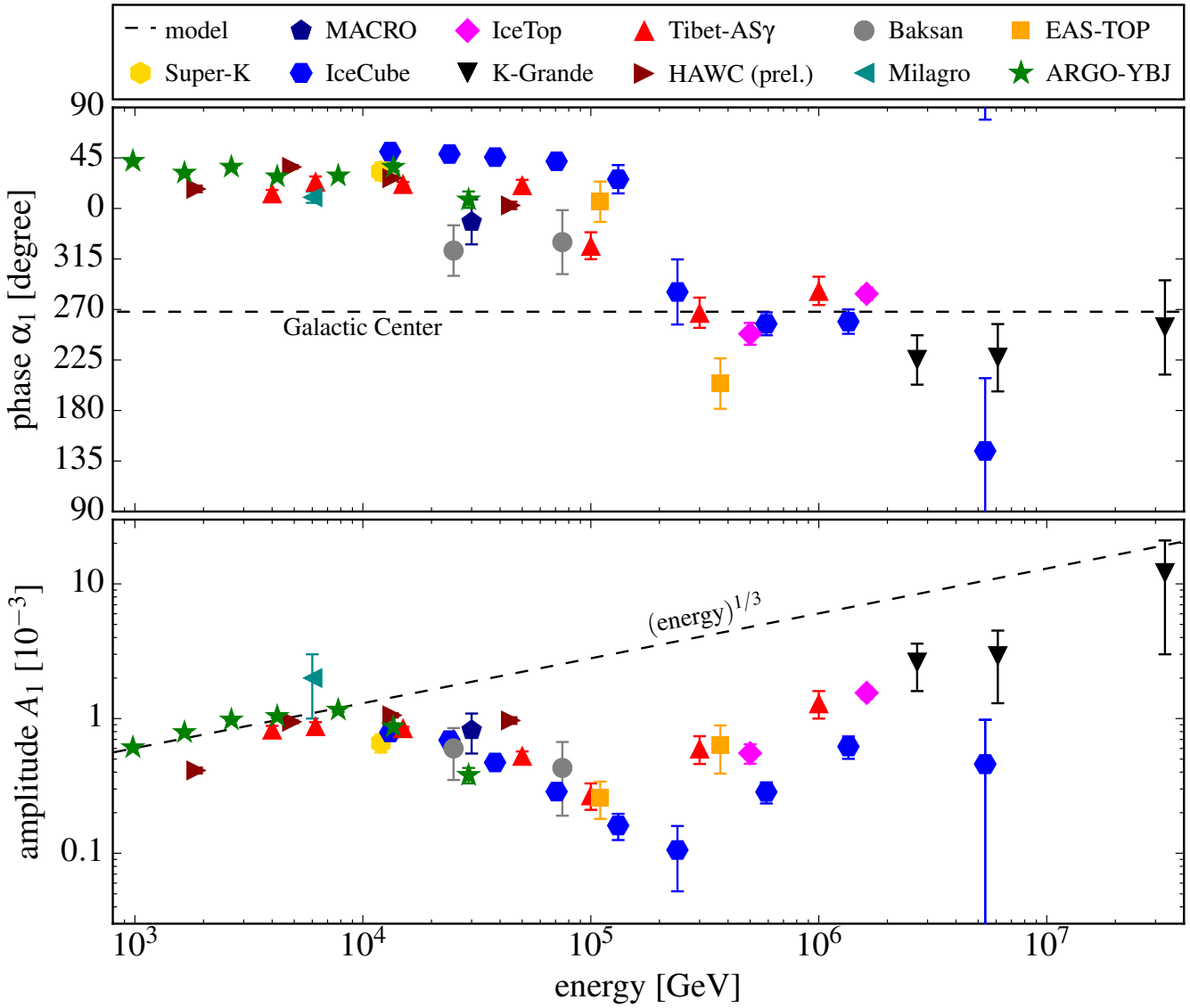

Galactic Center

Ahlers & Mertsch, Progress in Particle and Nuclear Physics (2016), in preparation

IceCube 7-year Data

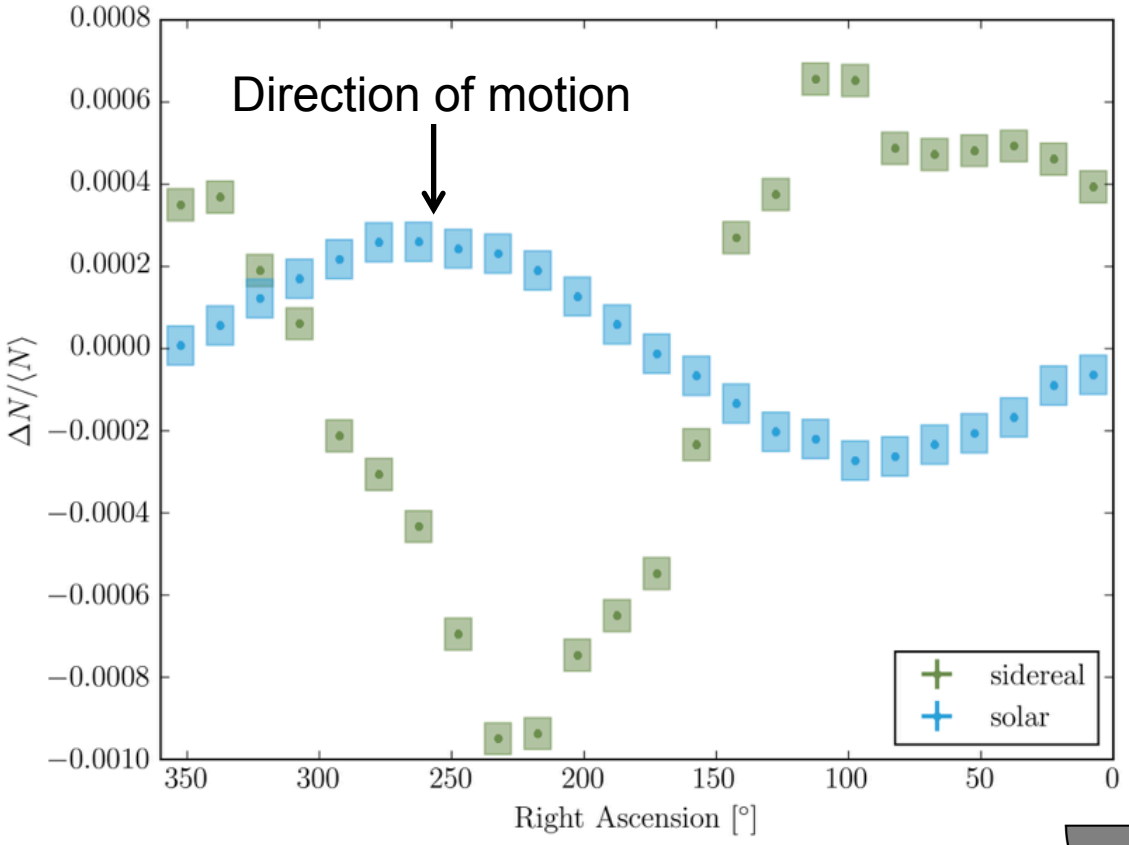

Sidereal anisotropy

Solar dipole

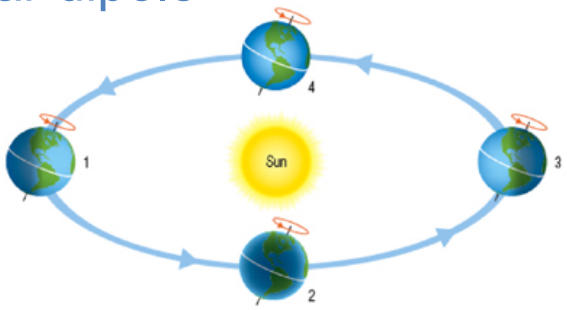

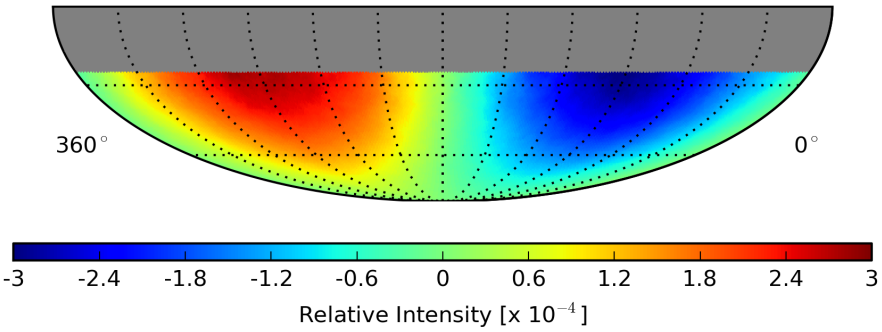

IceCube Collab.,
ApJ 826 (2016) 220 (+1 year of data)

Time Dependence

- Large-scale structure: no significant time variation in 7 years of IceCube data (2009–2016) and 7 years of AMANDA data (2000–2006) (arXiv:1309.7006)
  - 23rd solar cycle 1996 June to 2008 January
  - 24th solar cycle 2008 January, maximum 2014 April

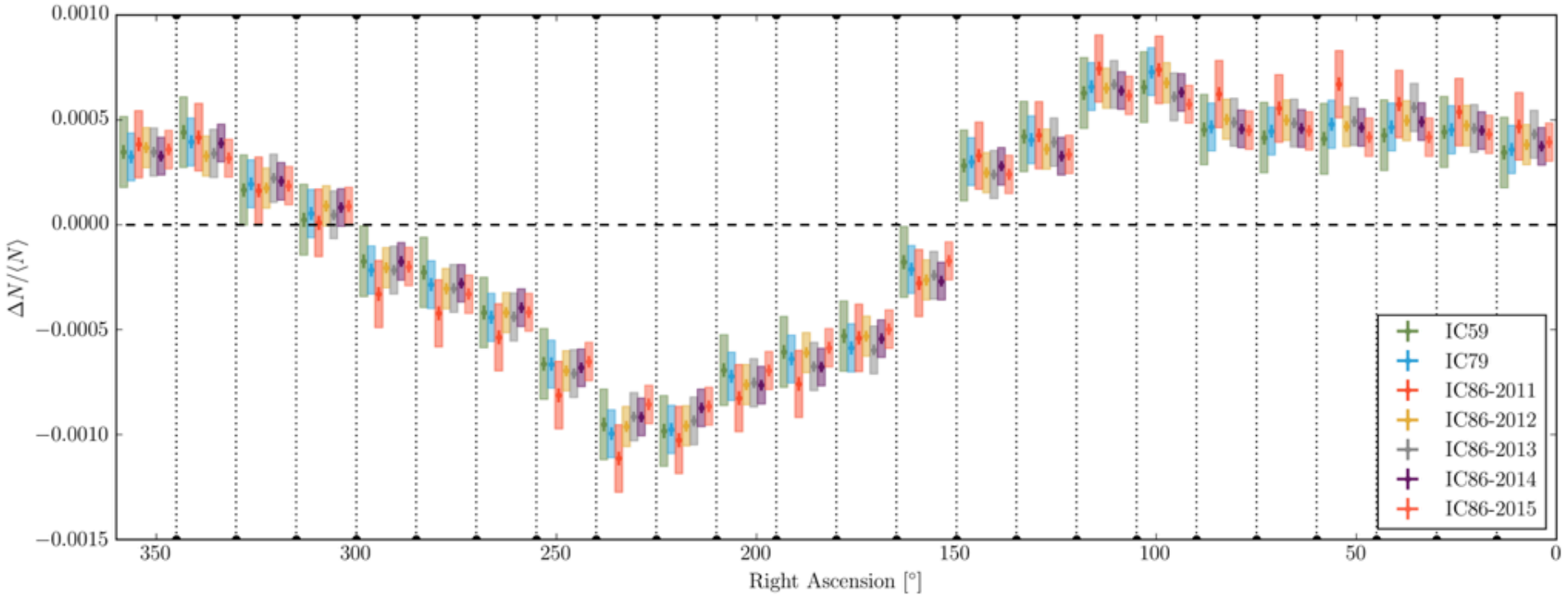

IceCube Collab.,
ApJ 826 (2016) 220 (+1 year of data)

Time Dependence

- Large-scale structure: no significant time variation in 9 years of data taken with the Tibet Air Shower Array (11/1999 to 12/2008) at 5 TeV.

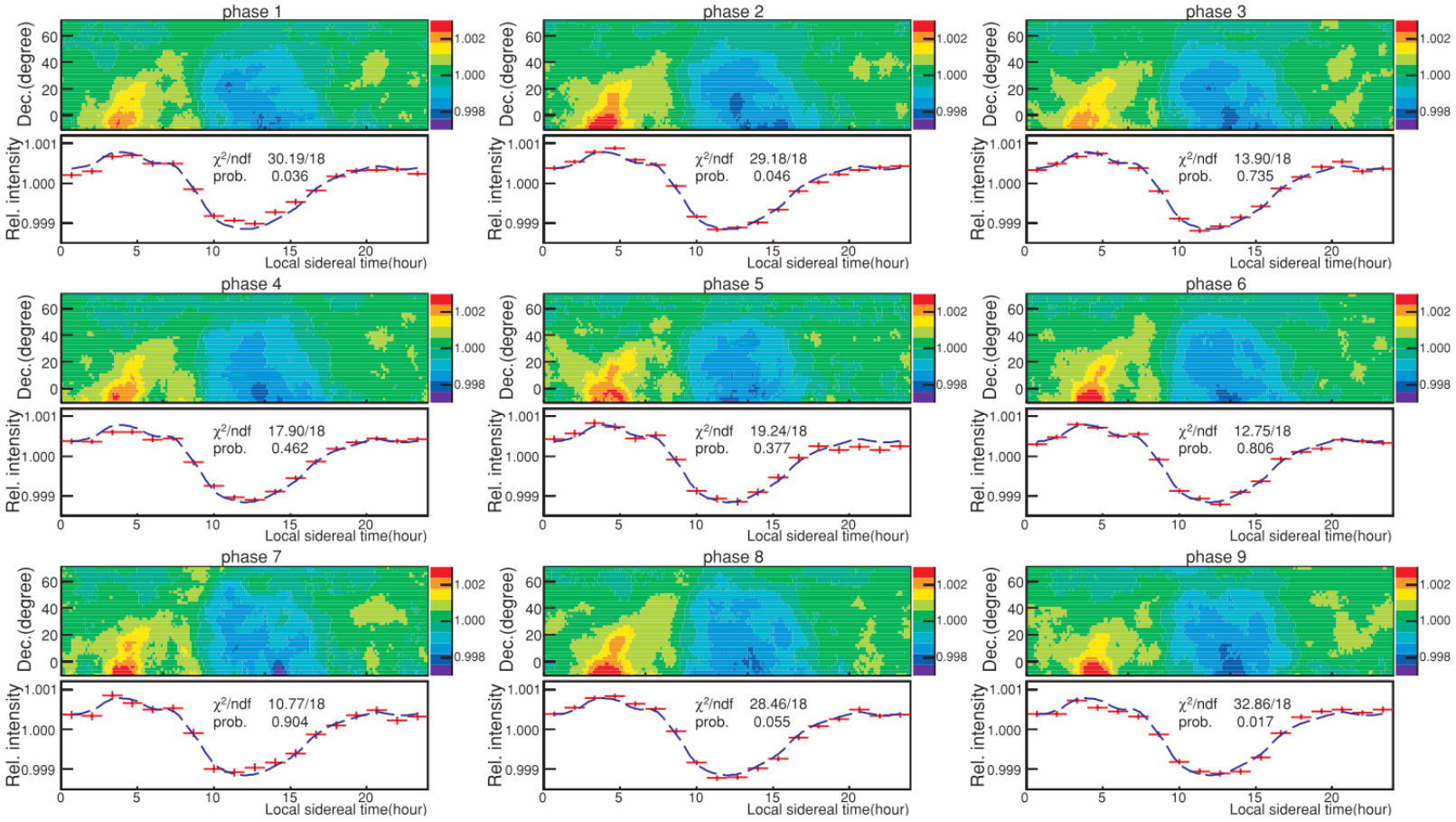

Tibet ASγ Collab.,
ApJ 711(2010) 119

Small-Scale Structure

ARGO-YBJ (2013)
PRD 88, 082001

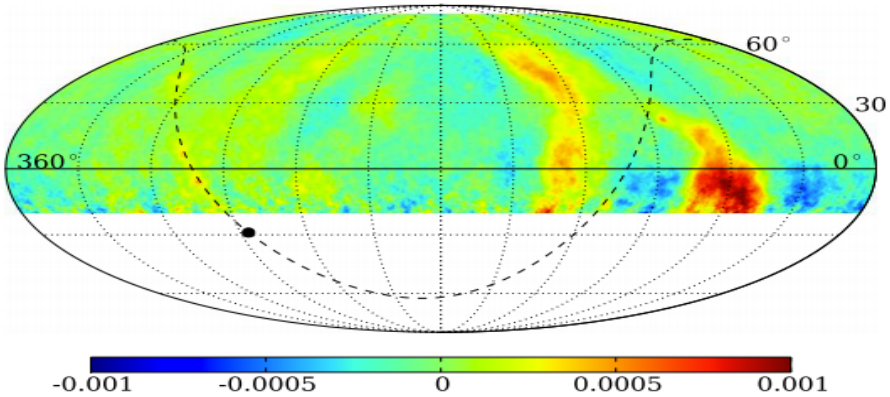

HAWC (2014)
ApJ 796, 108

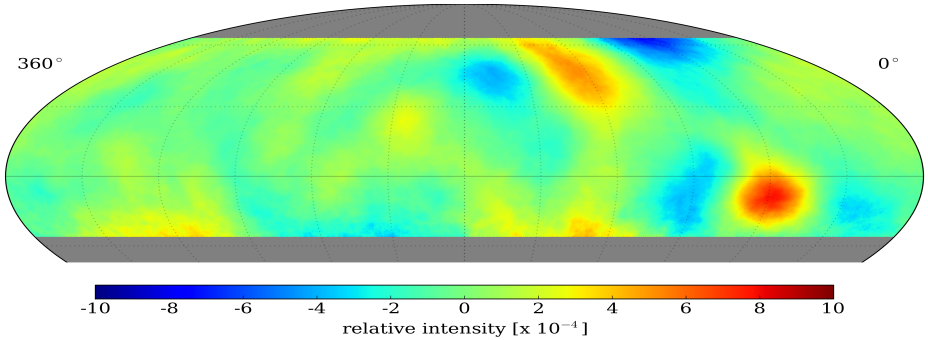

Milagro (2008)
PRL 101, 221101

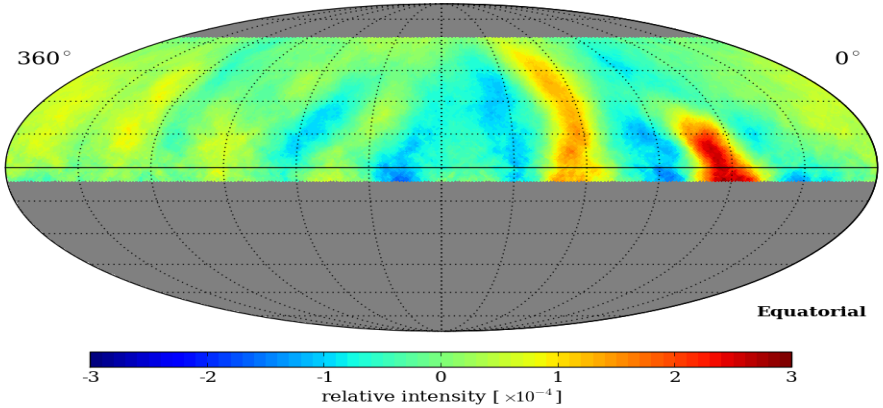

IceCube (2016)
ApJ 826, 220

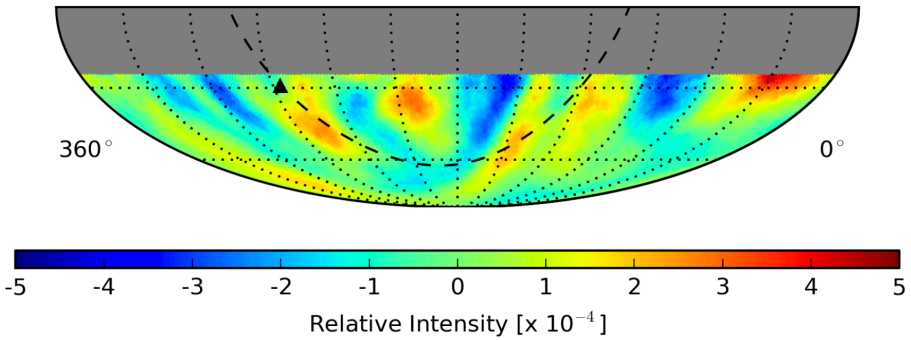

Small-Scale Structure

- Several significant excess regions. Region A is the strongest “source” on the HAWC sky map.
- Region A has an energy-dependent morphology and a harder spectrum than the isotropic cosmic-ray flux.

HAWC

ApJ 796 (2014) 108

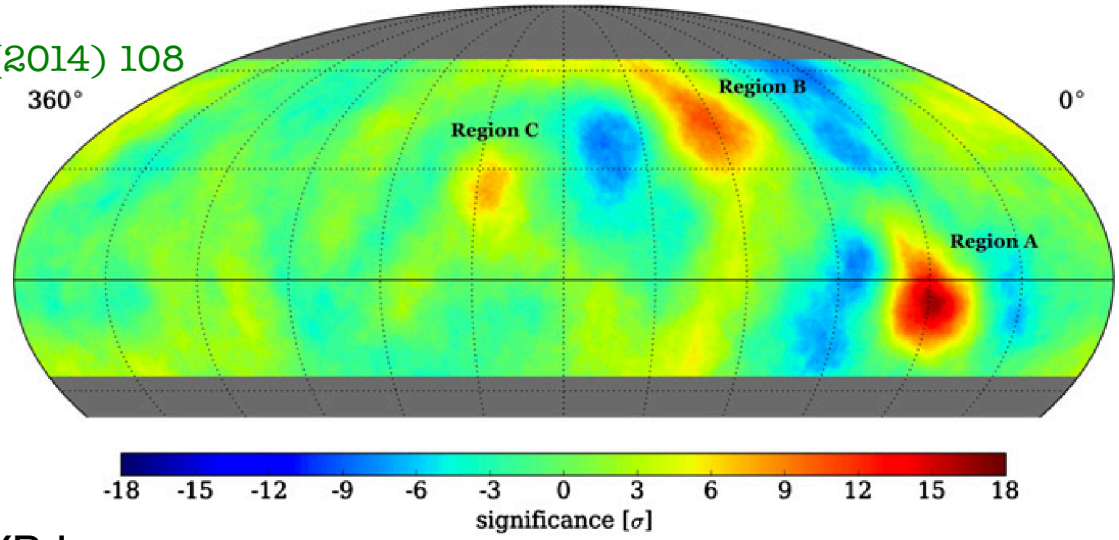

ARGO-YBJ

PRD 88 (2013) 082001

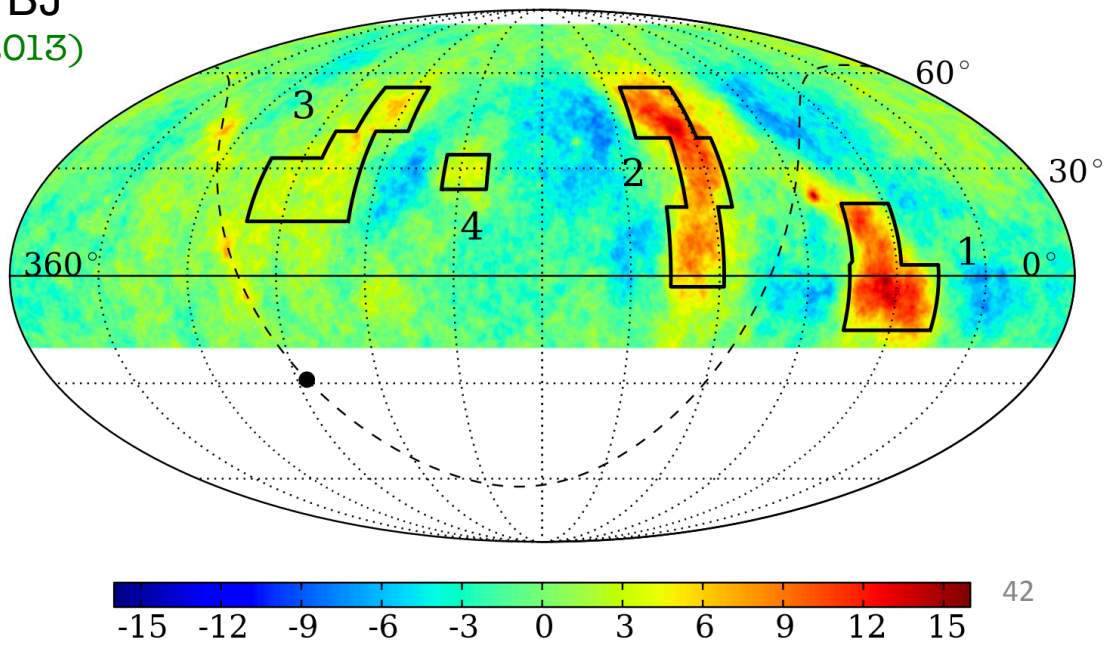

HAWC: Region A

- "Spectrum" of Region A in relative intensity in different energy proxy bins.
- Milagro and HAWC observe a harder spectrum compared to the isotropic cosmic-ray flux (~ 4σ effect in HAWC-100).

HAWC-100
ApJ 796 (2014) 108

Milagro
PRL 101, 221101

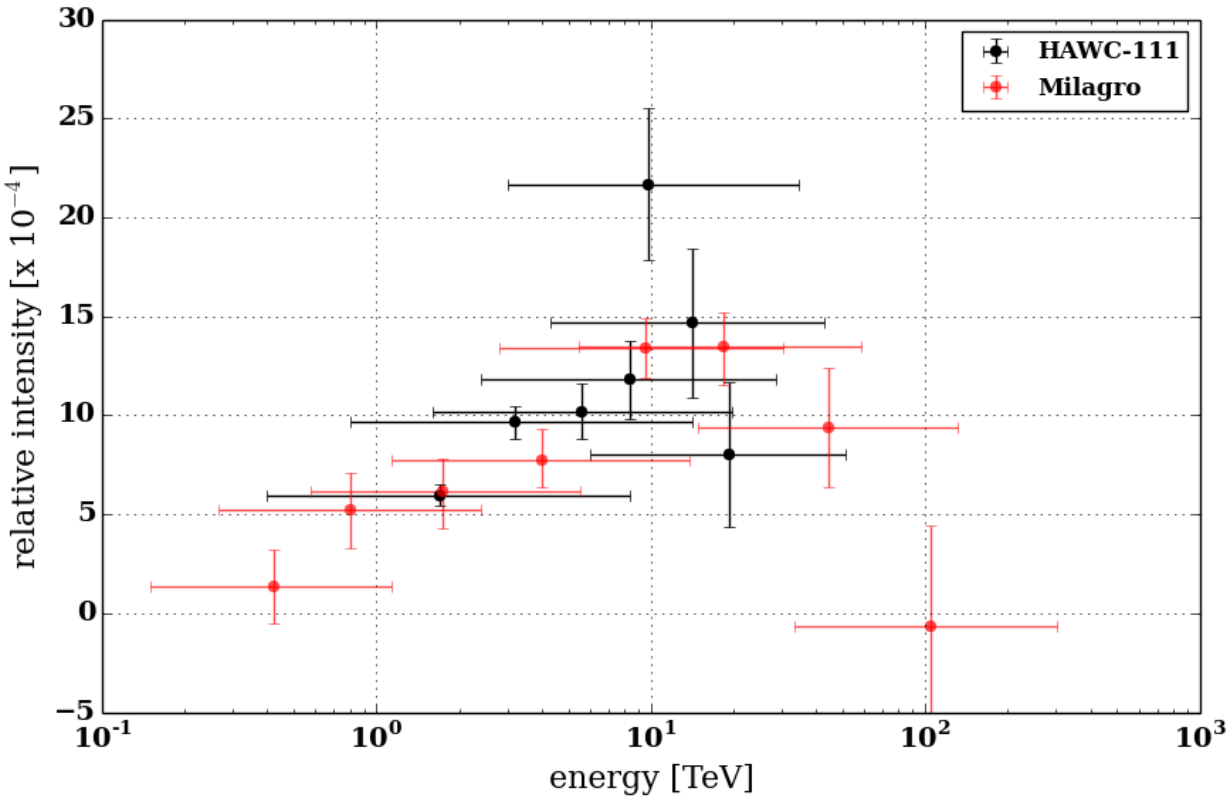

Energy Dependence

- Morphology of Region A is energy-dependent – it shifts northwards at higher energy (*top:* HAWC, *bottom:* ARGO-YBJ).

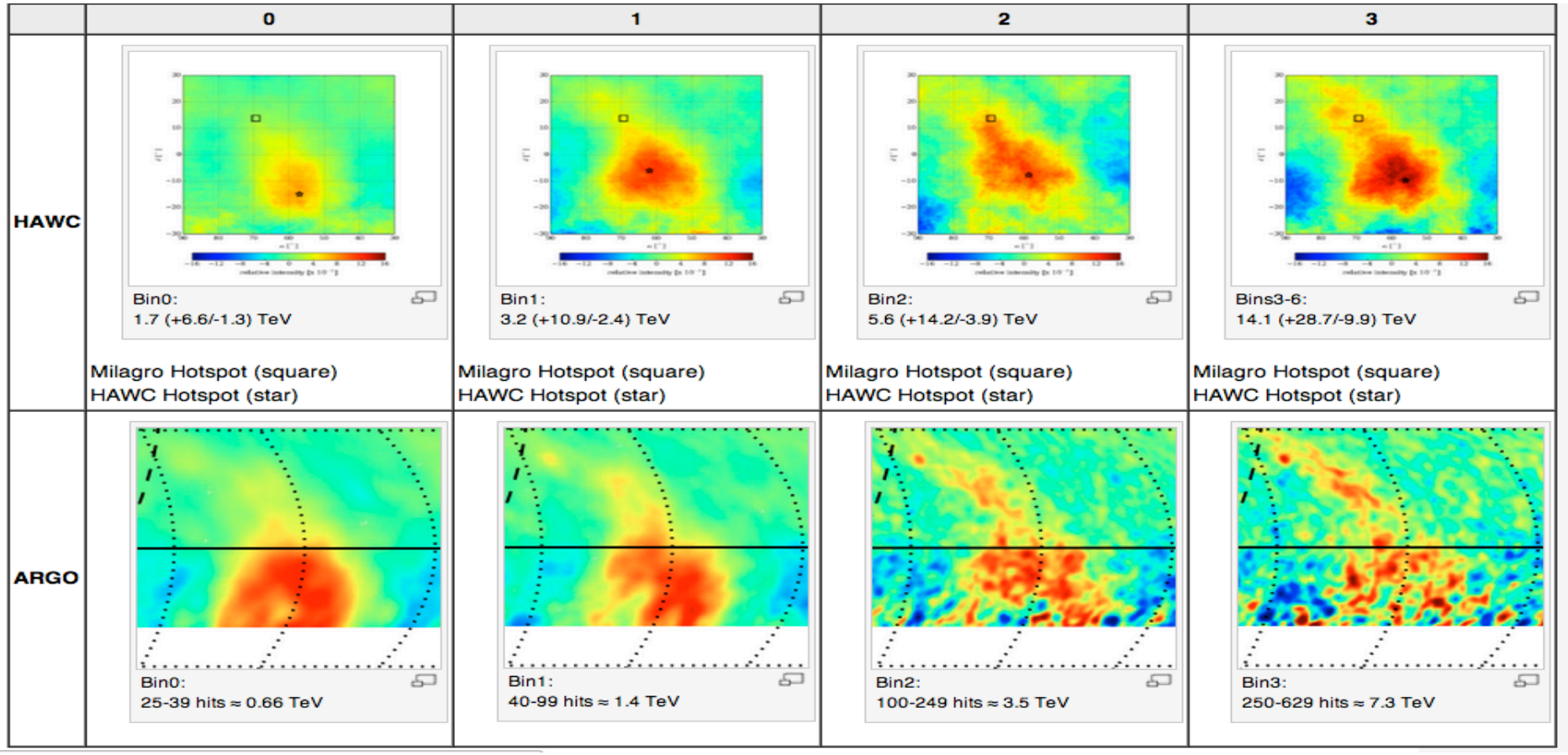

ARGO-YBJ: Region A

- Confirmed hard spectrum for Region A and cutoff around 10 TeV.
- Split Region into upper/lower part to study morphology change.
- Region shifts northward at higher energies.

Crab Nebula

Milagro Region A

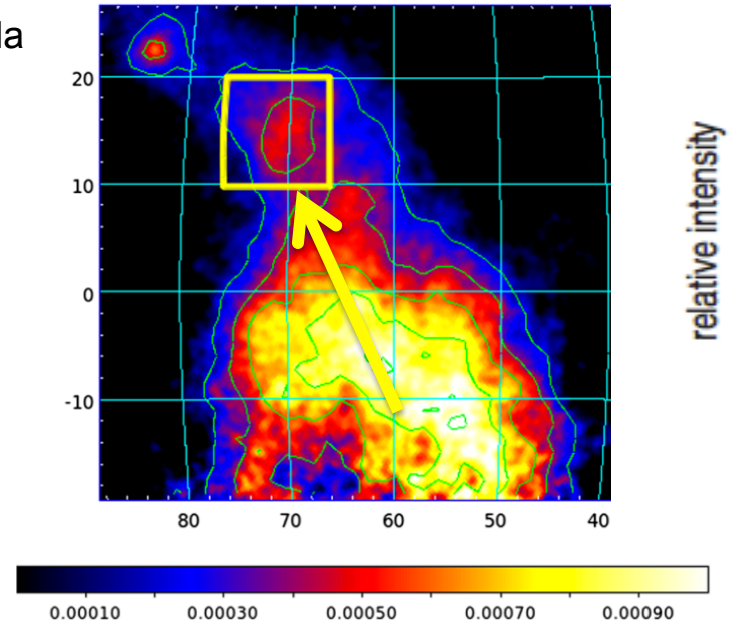

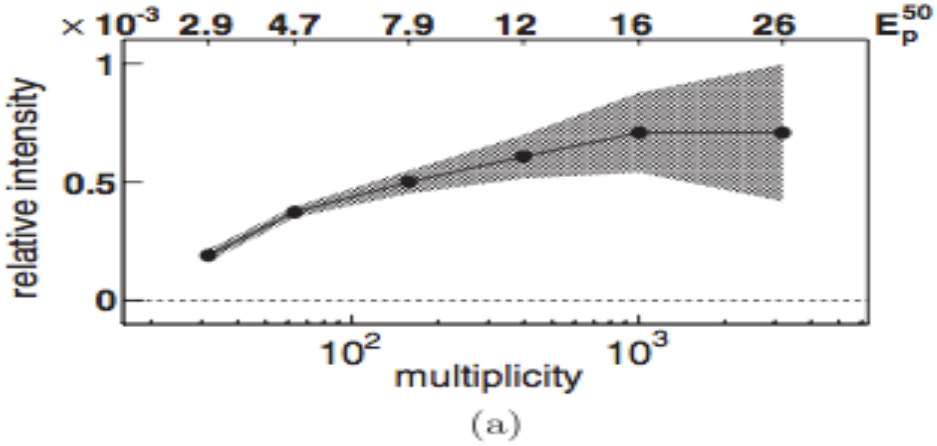

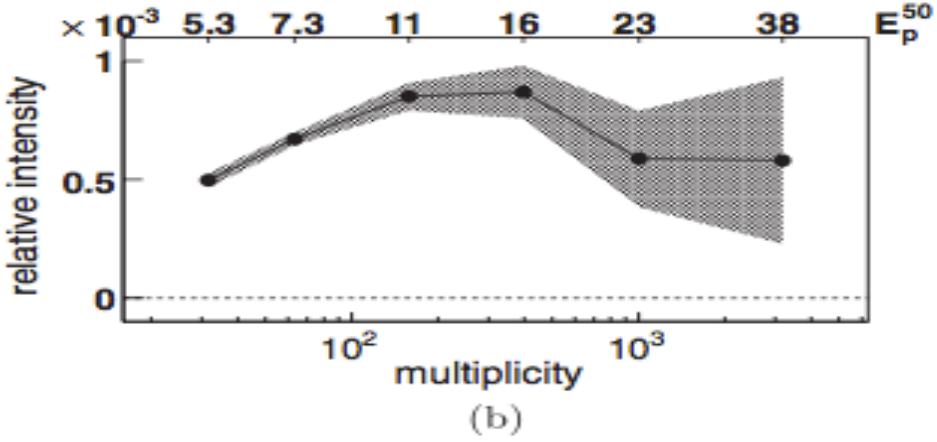

PRD 88 (2013) 082001

Time Dependence

- No significant time variation in small-scale anisotropy:
  - ARGO-YBJ (2007–2012)
  - IceCube (2009–2016) – power spectra of residual maps after subtraction of 7-year average from each year show no significant features.

ARGO-YBJ

PRD 88 (2013) 082001

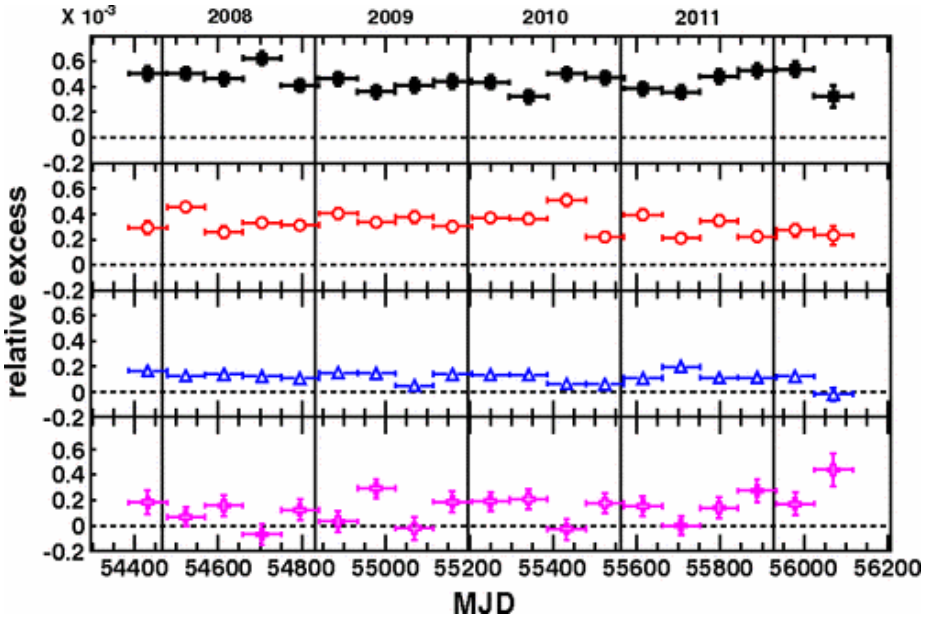

IceCube

ApJ 826 (2016) 220

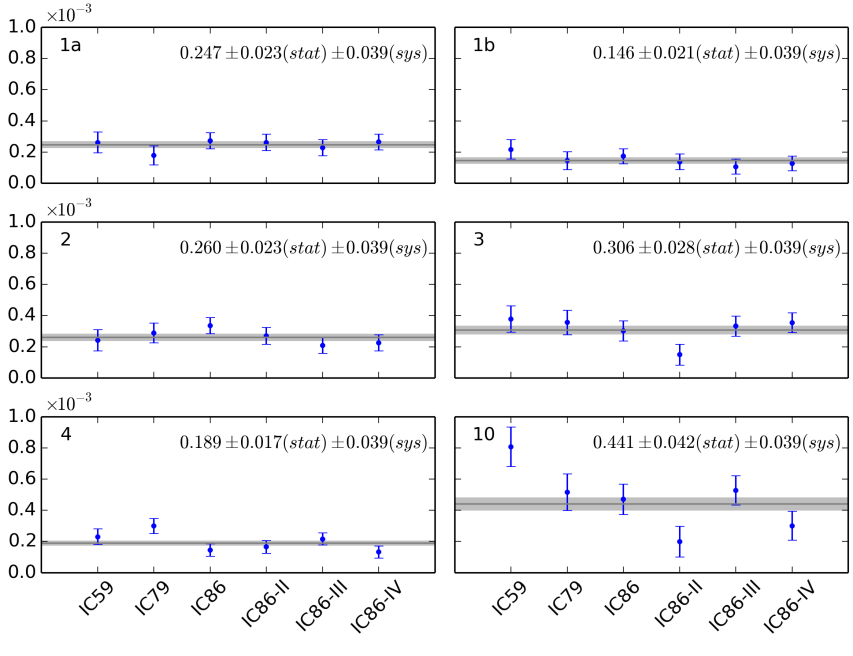

Anisotropy at E > 10 PeV

- At energies above several PeV, the increase in the amplitude of the anisotropy does not yet make up for the drop in flux.

- There are indications that the anisotropy persists up to several EeV:
  - Measurements of the phase in ordered energy intervals shows a transition at EeV

Pierre Auger Collab.,
Astropart. Phys. 34 (2011) 627
ICRC 2015 (arXiv:1509.03732)

IceCube/IceTop phase
at PeV energies

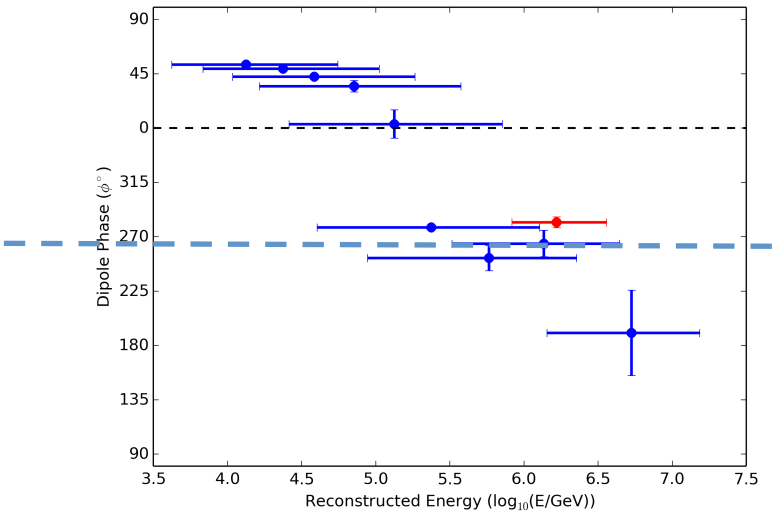

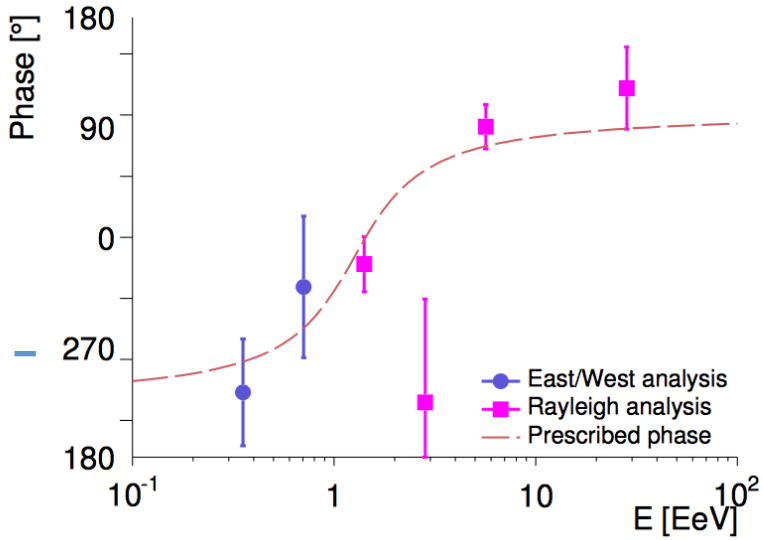

EeV Results

- Angular power spectrum and needlet wavelet analysis in the two energy ranges 4-8 EeV and > 8 EeV.
- Indication of a dipole moment in the > 8 EeV data ($p = 1.3 \times 10^{-5}$), consistent with previous results from Auger data and combined Auger+Telescope Array data.
- Dipole is pointing towards $(\alpha,\delta) = (97° \pm 16°, -39° \pm 17°)$.

Pierre Auger Collab.,
subm. to JCAP (arXiv:1611.06812)

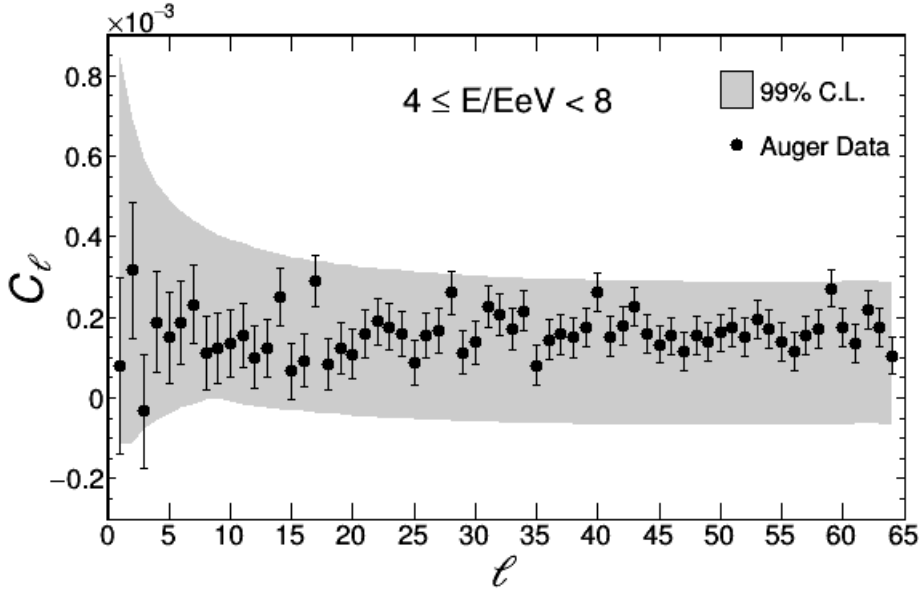

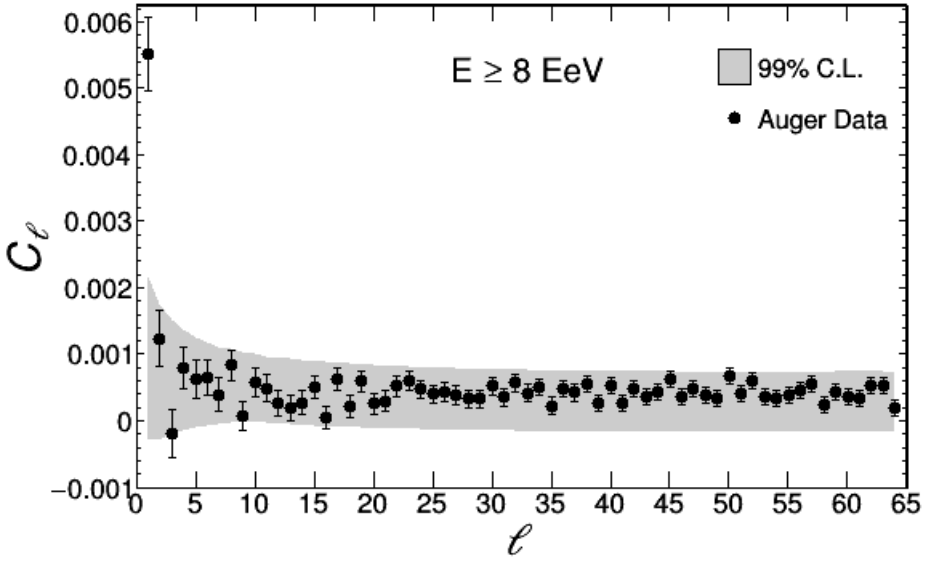

Summary and Outlook

- Anisotropy in the cosmic-ray arrival direction distribution at TeV to PeV energies is firmly established with data from a large number of instruments. The anisotropy…
  - … appears on all scales, from large-scales (dipole, quadrupole) to scales of the order of the angular resolution of the instruments.
  - … has a relative intensity of 10^{-3} to 10^{-5},
  - … is energy-dependent,
  - … has a complex morphology,
  - … does not appear to depend on time.

- Current analysis methods have known biases, and these should be taken into account when interpreting the experimental results.

- At the highest energies (> 8 EeV), the Pierre Auger Observatory starts to see significant dipole structure.

Summary and Outlook

Coming up:

- The HAWC and IceCube data sets are rapidly increasing in size.
- A combined analysis of IceCube/HAWC data can cover (almost) the entire sky and help to overcome systematic biases of the partial sky coverage of individual experiments. Matching the energy of the maps is, however, not trivial.
- IceTop has the potential for a combined anisotropy/energy spectrum/ chemical composition analysis at energies > PeV.